Supporting Information (SI)

Unveiling the fragmentation mechanisms of modified amino acids as the key for their targeted identification

Maricruz Mamani-Huanca[1], Ana Gradillas[1], Alberto Gil de la Fuente[1,2], Ángeles López-Gonzálvez[1], Coral Barbas[1*]

[1]Centre for Metabolomics and Bioanalysis (CEMBIO), Department of Chemistry and Biochemistry, , Facultad de Farmacia, Universidad San Pablo-CEU, CEU Universities, Urbanización Montepríncipe, 28660 Boadilla del Monte

[2]Department of Information Technology, Escuela Politécnica Superior, Universidad San Pablo-CEU, CEU Universities, Urbanización Montepríncipe, 28660 Boadilla del Monte

*Corresponding author: cbarbas@ceu.es

Supporting Information

Supporting Text for Experimental Section

Supporting Text for Figure 1

Supporting Tables S1-S3

Supporting Figures S1-S15

Supporting Spectra S1-S20

Compilation of all fragmentation spectra setting the fragmentor voltage at 100 and 200 V for 20 proteinogenic L-amino acids.

Spectra group 1: L-glycine, L-alanine, L-proline, L-valine, L-leucine and L-isoleucine

Spectra group 2: L-phenylalanine, L-tyrosine, L-histidine and L-tryptophan,

Spectra group 3: L-cysteine, L-methionine, L-asparagine and L-glutamine

Spectra group 4: L-serine, L-threonine, L-aspartic acid, L-glutamic acid

Spectra group 5: L-lysine and L-arginine

Supporting Text for Experimental Section

Chemicals

Ultrapure water used to prepare all aqueous solutions was obtained from Water Milli-Q 185 Plus system (Millipore, Bedford, USA). LC-MS-grade acetonitrile and methanol were purchased from Fluka Analytical (Sigma-Aldrich Chemie, Steinheim, Germany), sodium hydroxide solution 1 M was obtained from Agilent Technologies. MS-grade formic acid was obtained from Sigma-Aldrich. Purine and HP-0921 (hexakis(1H,1H,3H-tetrafluoropropoxy)phosphazene solution) both used as reference masses, were provided from Agilent Technologies. Methionine sulfone used as an internal standard (IS) was purchased from Sigma-Aldrich.

Collection of a set of 57 commercially available standards, including 20 proteinogenic L-AAs (Table S1), 19 modified L-AAs (Table S2) and other 18 related compounds (Table S3), were purchased from Sigma Aldrich.

Solutions, samples and their preparation

A solution of formic acid 1 M in 10% of methanol was used for the background electrolyte (BGE). The sheath liquid consisted of methanol-water (50:50) (v/v) and two reference masses (m/z ions 121.0508-purine and 922.0098-HP-0921). Solution of 0.2 M formic acid in 5% acetonitrile with 0.4 mM methionine sulfone was used in the preparation of samples prior to analysis. Fifty-seven standard solutions were prepared with concentrations of 25 mg/L with 0.2 mM of methionine sulfone.

Samples: A pooled plasma sample was purchased from Regional Centre for Transfusion Medicine (Bialystok, Poland). The urine sample was obtained from a female donor (University CEU San Pablo). Neutrophils, macrophages and *Leishmania donovani* sp. samples used were obtained from different metabolomics studies previously carried out in CEMBIO.

Plasma sample preparation was performed following a protocol previously developed by Naz et al.[1] Briefly, 100 µL of plasma sample were added with 100 µL of 0.2 M formic acid in 5% acetonitrile with 0.4 mM methionine sulfone, mixed for 1 min and transferred to a Centrifree® Ultrafiltration Device (30 kDa) (Millipore Ireland, Eire), which was then centrifuged at 2000 x *g* for 70 min at 4 °C in (Heraeus Megafuge 1.0R). The resulting filtrate was placed directly into the vial for analysis.

For urine sample preparation, 100 µL of urine was added with 100 µL of a solution of 0.2 M formic acid with 0.4 mM of methionine sulfone, it was vortex-mixed for 1 min, the solution was centrifuged at 600 x *g* for 15 min at 4 °C, 100 µL of supernatant were transferred to vials for their analysis.

Extraction of metabolites from neutrophils, macrophages and *Leishmania donovani* sp. samples were performed following the protocols previously described by Castilho-Martins et al.[2]

Data Handling

Extracted Ion Chromatograms (EIC) and spectra for each standard amino acid were obtained from MassHunter Qualitative software (B.08.00, Agilent Technologies). Relative migration time (RMT) for each compound was calculated with methionine sulfone as IS.[3]

Deconvolution of the raw data was performed using MassHunter Profinder software (B.08.00, Agilent Technologies) through the algorithm called Recursive Feature Extraction (RFE). This algorithm reprocesses data in two steps: first, it applies the Molecular Feature Extraction (MFE) algorithm, which performs feature extraction based on the isotopic distribution, presence of adducts, dimers and double charged-states; secondly, the RFE algorithm finds with high accuracy the extracted ion chromatogram so that the areas of the peaks can be integrated. Finally, it creates a list of all possible components, described by mass, migration time and abundance.

Peaks Identification

Because the signal of the compound of interest is often distributed over multiple entities in the mass spectrum (different isotopes, adducts, in-source fragments and even dimers), for peak identification it is important to rely on the RMT and peak shape of the extracted ion chromatograms (EICs) that correspond to the ions present in the average spectrum (Figure S12).[4]

Thus, a fragment is considered when it has the following characteristics: first, the same migration time than the protonated pseudo-molecular ion $[M+H]^+$; second, increased intensity with increased in-source voltage, and third, the same peak shape as the $[M+H]^+$.[5] Fragments of each compound were compared with the results of a previous correlation analysis described in CEMBIO which used Pearson product-moment and Spearman-rank methods for calculating the correlation coefficients. [6]

On the other hand, the accurate mass obtained was matched to compounds from web-based sources and compared with the MS/MS spectra available from the databases METLIN (http://metlin.scripps.edu) and HMDB (http://hmdb.ca). Ions produced by the in-source fragmentation process were similar to those observed by low-energy MS/MS CID processes. The spectra were not identical but usually complementary.[7]

Supporting Text for Figure 1

Protonation site in the AA core: There are three main sites of protonation available: the α-amino nitrogen, the carbonyl oxygen (CO) and the hydroxyl oxygen (OH). It has been postulated that the formation of the characteristic immonium ion starts with the protonation site on the nitrogen atom of the α–amino from the AA core, which is the most stable protonated form; afterwards, a proton is rapidly transferred to the hydroxyl group. The exception for this is L-HisH$^+$, which is the only aromatic AA that protonates on the side chain; in this case, a proton is transferred from the protonated nitrogen in the more basic imidazole ring to the hydroxyl of the carboxylic acid, which is required prior to the elimination of H_2O (Figure 1).[8]

Then, when the oxygen atom of the hydroxyl group is protonated, it leads, by a simple cleavage bond, to a neutral loss of H_2O (-18.0106 Da), yielding an acylium ion which then loses CO (-27.9949 Da) by rearrangement of the α-amino group. All the evidences [8] indicate that the acylium ions formed by elimination of H_2O are unstable and exothermically eliminate CO to form $[M+H-H_2O-CO]^+$. Thus, the formation of the fragment $[M+H-H_2O-CO]^+$ is not produced either from $[M+H-H_2O]^+$ or $[M+H-CO]^+$, it should be directly generated from $[M+H]^+$ (Figure 1, Pathway a.1.). This well-known sequential loss of two neutral species (H_2O+CO), without detecting any intermediate, to form the characteristic **immonium ion** is the common reaction observed as a major fragmentation reaction for all AAH$^+$, except L-TrpH$^+$, L-LysH$^+$ and L-ArgH$^+$. We confirmed this with our experimental data. For L-LysH$^+$ and L-ArgH$^+$ the immonium ion was never observed (Table S1 and Figures S3-S7).[8]

Identity of the side-chain group (R): With the exception of L-ProH$^+$, L-SerH$^+$, L-ThrH$^+$, L-AspH$^+$ and L-GluH$^+$, all the AAs lose ammonia (-NH_3). This important loss is not only from the immonium ion to form fragment $[M+H-H_2O-CO-NH_3]^+$ (Figure 1, Pathway a.1.) but also as a loss by direct cleavage assisted by the side-chain, a displacement reaction to form fragment $[M+H-NH_3]^+$ (Figure 1, Pathway a.2.). The formation mechanism of $[M+H-NH_3]^+$ from $[M+H]^+$ is due to a rearrangement between the side-chain group and the protonated α-amino group. The process is initiated by a nucleophilic attack of the backbone on the side chain to the Cα, which initiates the elimination of NH_3 and the formation of a three-, four or five-membered ring intermediate. An intramolecular H^+ transfer is involved in the further loss of H_2O from the α-carbohydroxy group, accompanied finally by the loss of CO to yield the DI fragment $[M+H-NH_3-H_2O-CO]^+$. Many computational studies have demonstrated that the competition between the two above-mentioned fragmentation pathways for each AAH$^+$ are governed by a combination of enthalpy factors and activation barriers associated with cyclization-rearrangements. Recent studies carried out by Choi *et al.* have helped us understand these **ring-system-based fragmentation mechanisms**.[9] As a result, the formation of the

immonium ion, $[M+H-H_2O-CO]^+$, can be in competition with the loss of NH_3, $[M+H-NH_3]^+$, by direct cleavage assisted by the side-chain for several AAs bearing a functional group on the side-chain (Figure 1, Pathways a.1., a.2. and Table S1).

In the course of our mechanistic study we have observed an unusual fragmentation pathway whose plausible mechanism was proven in previous investigations and where the chemistry is dominated by the elimination of the α-amino group as a neutral loss (Figure 1, Pathway a.3). [10]

***Protonation site in the side-chain functional group*:** When protonation site is on a basic atom on the side-chain group, a good leaving group ($-H_2O$, $-NH_3$, -amidine or -guanidine) is often observed (Figure 1, Pathway b and Table S1).

References

1. Naz, S.; Garcia, A.; Rusak, M.; Barbas, C., Method development and validation for rat serum fingerprinting with CE-MS: Application to ventilator-induced-lung-injury study. *Anal. Bioanal. Chem.* **2013,** *405* (14), 4849-4858.
2. Castilho-Martins, E. A.; Canuto, G. A. B.; Muxel, S. M.; Laranjeira da Silva, M. F.; Floeter-Winter, L. M.; del Aguila, C.; Lopez-Gonzalvez, A.; Barbas, C., Capillary electrophoresis reveals polyamine metabolism modulation in *Leishmania (Leishmania) amazonensis* wild-type and arginase-knockout mutants under arginine starvation. *Electrophoresis* **2015,** *36* (18), 2314-2323.
3. Soga, T.; Ohashi, Y.; Ueno, Y.; Naraoka, H.; Tomita, M.; Nishioka, T., Quantitative Metabolome Analysis Using Capillary Electrophoresis Mass Spectrometry. *J. Proteome Res.* **2003,** *2* (5), 488-494.
4. De Vijlder, T.; Valkenborg, D.; Lemière, F.; Romijn, E. P.; Laukens, K.; Cuyckens, F., A tutorial in small molecule identification via electrospray ionization-mass spectrometry: The practical art of structural elucidation. *Mass. Spectrom. Rev.* **2018,** *37* (5), 607-629.
5. Domingo-Almenara, X.; Montenegro-Burke, J. R.; Guijas, C.; Majumder, E. L. W.; Benton, H. P.; Siuzdak, G., Autonomous METLIN-Guided In-source Fragment Annotation for Untargeted Metabolomics. *Anal. Chem.* **2019,** *91* (5), 3246-3253.
6. Godzien, J.; Armitage, E. G.; Angulo, S.; Paz Martinez-Alcazar, M.; Alonso-Herranz, V.; Otero, A.; Lopez-Gonzalvez, A.; Barbas, C., In-source fragmentation and correlation analysis as tools for metabolite identification exemplified with CE-TOF untargeted metabolomics. *Electrophoresis* **2015,** *36* (18), 2188-2195.
7. Parcher, J. F.; Wang, M.; Chittiboyina, A. G.; Khan, I. A., In-source collision-induced dissociation (IS-CID): Applications, issues and structure elucidation with single-stage mass analyzers. *Drug. Test. Anal.* **2018,** *10* (1), 28-36.
8. El Aribi, H.; Orlova, G.; Hopkinson, A. C.; Siu, K. W. M., Gas-phase fragmentation reactions of protonated aromatic amino acids: Concomitant and consecutive neutral eliminations and radical cation formations. *J. Phys. Chem. A* **2004,** *108* (17), 3844-3853.

9. Choi, S. S.; Song, M. J.; Kim, O. B.; Kim, Y., Fragmentation patterns of protonated amino acids formed by atmospheric pressure chemical ionization. *Rapid Commun. Mass Spectrom.* **2013,** *27* (1), 143-151.
10. Shek, P. Y. I.; Zhao, J.; Ke, Y.; Siu, K. W. M.; Hopkinson, A. C., Fragmentations of protonated arginine, lysine and their methylated derivatives: Concomitant losses of carbon monoxide or carbon dioxide and an amine. *J. Phys. Chem. A* **2006,** *110* (27), 8282-8296.
11. Zhang, P.; Chan, W.; Ang, I. L.; Wei, R.; Lam, M. M. T.; Lei, K. M. K.; Poon, T. C. W., Revisiting Fragmentation Reactions of Protonated α-Amino Acids by High-Resolution Electrospray Ionization Tandem Mass Spectrometry with Collision-Induced Dissociation. *Scientific Reports* **2019,** *9* (1).
12. Dookeran, N. N.; Yalcin, T.; Harrison, A. G., Fragmentation reactions of protonated α-amino acids. *J. Mass Spectrom.* **1996,** *31* (5), 500-508.
13. Rogalewicz, F.; Hoppilliard, Y.; Ohanessian, G., Fragmentation mechanisms of α-amino acids protonated under electrospray ionization: A collisional activation and ab initio theoretical study. *Int. J. Mass Spectrom.* **2000,** *195-196*, 565-590.
14. Zhao, J.; Shoeib, T.; Siu, K. W. M.; Hopkinson, A. C., The fragmentation of protonated tyrosine and iodotyrosines: The effect of substituents on the losses of NH_3 and of H_2O and CO. *Int. J. Mass Spectrom.* **2006,** *255-256* (1-3), 265-278.
15. 15. Lioe, H.; O'Hair, R. A. J.; Reid, G. E., Gas-phase reactions of protonated tryptophan. *Journal of the American Society for Mass Spectrometry* **2004,** *15* (1), 65-76.
16. Sumner, L. W.; Amberg, A.; Barrett, D.; Beale, M. H.; Beger, R.; Daykin, C. A.; Fan, T. W.; Fiehn, O.; Goodacre, R.; Griffin, J. L.; Hankemeier, T.; Hardy, N.; Harnly, J.; Higashi, R.; Kopka, J.; Lane, A. N.; Lindon, J. C.; Marriott, P.; Nicholls, A. W.; Reily, M. D.; Thaden, J. J.; Viant, M. R., Proposed minimum reporting standards for chemical analysis Chemical Analysis Working Group (CAWG) Metabolomics Standards Initiative (MSI). *Metabolomics* **2007,** *3* (3), 211-221.
17. Schrimpe-Rutledge, A. C.; Codreanu, S. G.; Sherrod, S. D.; McLean, J. A., Untargeted Metabolomics Strategies-Challenges and Emerging Directions. *J Am Soc Mass Spectrom* **2016,** *27* (12), 1897-1905.

Table S1. Fragments results for 20 proteinogenic L-aminoacids.

Amino acids	Symbol AAs	RMT	Molecular formula	Monoisotopic mass	AAH^+ $[M+H]^+$	All Fragments to 200 V
Aliphatic - GROUP 1.						
L-glycine	**L-Gly**	0.76	$C_2H_5NO_2$	75.0320	76.0392	fragments with ***m/z*** less than 50 Da
L-alanine	**L-Ala**	0.81	$C_3H_7NO_2$	89.0477	90.0548	fragments with ***m/z*** less than 50 Da
L-proline	**L-Pro**	0.93	$C_5H_9NO_2$	115.0633	116.0706	**70.0658**, 68.0497
L-valine	**L-Val**	0.87	$C_5H_{11}NO_2$	117.0790	118.0860	**72.0808**, 57.0578, 55.0546
L-leucine	**L-Leu**	0.89	$C_6H_{13}NO_2$	131.0946	132.1015	**86.0972**, 69.0707
L-isoleucine	**L-Ile**	0.89	$C_6H_{13}NO_2$	131.0946	132.1013	**86.0972**, 69.0708
Aromatic - GROUP 2.						
L-histidine	**L-His**	0.69	$C_6H_9N_3O_2$	155.0695	156.0761	139.0514, **110.0709**, 95.0609, 93.0453, 83.0613, 82.0531, 81.0454, 69.0461, 68.0503, 66.0350, 56.0507
L-phenylalanine	**L-Phe**	0.94	$C_9H_{11}NO_2$	165.0790	166.0836	149.0578, 131.0474, **120.0784**, 119.0716, 107.0479, 105.0445, 103.0531, 102.0454, 93.0687, 91.0531, 79.0534, 77.0377, 65.0380
L-tyrosine	**L-Tyr**	0.96	$C_9H_{11}NO_3$	181.0739	182.0816	165.0525, 147.0419, **136.0737**, 123.0422, 119.0472, 95.0474, 91.0527
L-tryptophan	**L-Trp**	0.94	$C_{11}H_{12}N_2O_2$	204.0899	205.0974	**188.0711**, 170.0602, 159.0918, 146.0603, 144.0808, 142.0634, 132.0809,130.0604, 118.06540, 91.0546
Sulfur - containing and Amidic - GROUP 3.						
L-cysteine	**L-Cys**	0.95	$C_3H_7NO_2S$	121.0198	122.0264	105.0013, 86.9903, **76.0224**, **58.9956**
L-asparagine	**L-Asn**	0.91	$C_4H_8N_2O_3$	132.0535	133.0602	116.0342, **87.0556**, 74.0242[(a)], **70.0293**
L-glutamine	**L-Gln**	0.92	$C_5H_{10}N_2O_3$	146.0691	147.0756	130.0498, 102.0555, 101.0713, **84.0447**, 64.0165, 56.0503
L-methionine	**L-Met**	0.92	$C_5H_{11}NO_2S$	149.0511	150.0583	**133.0319**, **104.0531**, 102.0553, 87.0268, 74.0243, 74.0597, 61.0115, 56.0503
Hydroxy and Acidic - GROUP 4.						
L-serine	**L-Ser**	0.88	$C_3H_7NO_3$	105.0426	106.0499	88.0397, 70.0291, **60.0453**
L-threonine	**L-Thr**	0.91	$C_4H_9NO_3$	119.0582	120.0653	**102.0551**, 84.0448, **74.0607**, 56.0502
L-aspartic acid	**L-Asp**	0.97	$C_4H_7NO_4$	133.0375	134.0443	116.0350, **88.0398**, 74.0242[(a)], **70.0296**
L-glutamic acid	**L-Glu**	0.94	$C_5H_9NO_4$	147.0532	148.0607	130.0497, 102.0553, **84.0450**, 56.0502
Basic - GROUP 5.						
L-lysine	**L-Lys**	0.65	$C_6H_{14}N_2O_2$	146.1055	147.1128	130.0863, 112.0766, 102.0914, **84.0811**, 67.0549, 56.0474
L-arginine	**L-Arg**	0.67	$C_6H_{14}N_4O_2$	174.1117	**175.1183**	158.0926, 130.0979, 116.0707, **70.0658**, 60.0563

m/z values for the **diagnostic ion** are given in bold type. [(a)] *m/z* intense but not diagnostic ion.

Table S1. Compilation of all fragmentation data setting the fragmentor voltage at 200 V in a CE-ESI(+)-TOF-MS system for 20 proteinogenic L-amino acids authentic standards. AAs were divided into five groups according to the typical fragments ions generated from AAH^+ based on their molecule-specific fragmentation behaviors and according to the reactivity of their side chain. All fragments from ISF-CID in accordance with fragments of protonated AAs investigated using HR-ESI-MS/MS with CID. [11]

Table S2. Fragments results for 19 modified L-amino acids.

				Fragmentation pattern observed for studied compounds (fragmentor voltage set at 200 V)[a]			
Compound Name	RMT	Molecular formula	Monoisotopic mass	$[M+H]^+$	Fragment diagnostic ion[b]	Fragment diagnostic ion + R[c]	Other fragments observe
modified-AAs GROUP 1							
***N*$_2$-methyl-L-glycine**	0.83	$C_3H_7NO_2$	89.0477	**90.0554**	n.d.	n.d.	n.d.
***N*$_2$-methyl-L-alanine**	0.87	$C_4H_9NO_2$	103.0633	104.0710	n.d.	n.d.	86.0600, 73.0284, 60.0808, **58.0651**
***N*$_2$,*N*$_2$-dimethylglycine**	0.94	$C_4H_9NO_2$	103.0633	104.0706	n.d.	n.d.	**58.0660**
***N*-methyl-L-proline**	1.03	$C_6H_{11}NO_2$	129.0790	130.0863	n.d.	**84.0811**	82.0653, 69.0578, 67.0394
***N*$_2$-acetyl-L-alanine**	1.99	$C_5H_9NO_3$	131.0582	132.0655	n.d.	n.d.	**90.0550**
***N*$_2$-methyl-L-isoleucine**	0.97	$C_7H_{15}NO_2$	145.1103	146.1176	86.0972	**100.1119**	128.1071, 85.0886, 71.0736, 70.0662, 69.0705, 58.0659
modified-AAs GROUP 2							
***N*$_2$-acetyl-L-tyrosine**	1.62	$C_{11}H_{13}NO_4$	223.0845	224.0904	**136.0747**	178.0846	210.1122, 206.0827, 196.0964, 193.0856, 182.0797, 165.0527, 151.0749, 147.0420, 119.0500, 91.0538
3-methyl-L-histidine	0.70	$C_7H_{11}N_3O_2$	169.0851	**170.0924**		124.0866	153.0660, 126.1026, 125.0710, 109.0763, 96.0687, 96.0659, 95.0605, 83.0612, 81.0445, 68.0502
1-methyl-L-histidine	0.70	$C_7H_{11}N_3O_2$	169.0851	170.0924		**124.0869**	126.1011, 110.0782, 109.0758, 97.076, 96.0683, 83.0607, 81.0451, 68.0468
modified-AAs GROUP 3							
S-methyl-L-cysteine	0.97	$C_4H_9NO_2S$	135.0354	136.0426	n.d.	90.0374	**119.0161**, 77.0060, 75.0258
***N*$_2$-acetyl-L-glutamine**	1.61	$C_7H_{12}N_2O_4$	188.0800	189.0873	**84.0444**	147.0747	172.0603, 130.0496, 129.0653, 101.0705
modified-AAs GROUP 4							
***N*$_2$-methyl-L-threonine**	1.07	$C_5H_{11}NO_3$	133.0740	134.0808	74.0619	88.0760	116.0707, 98.0605, 88.0760, 75.0310, 72.0809, **70.0660**, 60.0455, 57.0514
modified-AAs GROUP 5	RMT	Molecular formula	Monoisotopic mass	$[M+H]^+$	Fragment diagnostic ion[b]	Fragment diagnostic ion + R_n[c]	Other fragments observe
***N*$_2$-methyl-L-lysine**	0.74	$C_7H_{16}N_2O_2$	160.1212	161.1285	84.0816	**98.0962**	144.1023, 130.0864, 116.1080, 115.1232, 112.0759, 87.0450, 86.0611, 70.0657, 67.0547, 58.0657, 56.0504
***N*$_6$-methyl-L-lysine**	0.70	$C_7H_{16}N_2O_2$	160.1212	161.1285	**84.0816**	98.0962	144.1021, 130.0864, 126.0922, 116.1073, 115.1232, 112.0767, 70.0660, 67.0549, 65.0389
***N*$_6$,*N*$_6$-dimethyl-L-lysine**	0.72	$C_8H_{18}N_2O_2$	174.1368	**175.1441**	84.0809	n.d.	158.1174, 130.0863, 114.1275, 67.0547
***N*$_6$-acetyl-L-lysine**	0.84	$C_8H_{16}N_2O_3$	188.1161	189.1224	**84.0810**	126.0908	172.0968, 153.1024, 147.1132, 130.0852, 129.1025, 112.0753, 102.0924, 101.1078, 67.0546
***N*$_6$, *N*$_6$, *N*$_6$-trimethyl-L-lysine**	0.72	$C_9H_{20}N_2O_2$	188.1525	**189.1598**	84.0813	n.d.	144.1378, 130.0863, 128.1426
***N*$_G$,*N*$_G$-dimethyl-L-arginine**	0.71	$C_8H_{18}N_4O_2$	202.1430	**203.1497**	70.0659	n.d.	186.1248, 158.1289, 133.0967, 116.0708, 115.0863, 88.0874
***N*$_G$,*N*$_G$'-dimethyl-L-arginine**	0.72	$C_8H_{18}N_4O_2$	202.1430	**203.1497**	70.0659	n.d.	186.1248, 172.1080, 158.1289, 133.0967, 116.0708, 115.0863, 88.0870

[a] m/z values for the **base peak** are given in bold type.
[b] Diagnostic ions presented in Table 1 and discussed in Figures S3-7.
[c] **R** = + Methyl (+ 14.0157 Da), **R** = + Acetyl (+ 42.0106 Da) Li, L. et al. MyCompoundID: Using an evidence-based metabolome library for metabolite identification (https://pubs.acs.org/doi/abs/10.1021/ac400099b) n.d. not detected.

Table S2. Compilation of all fragmentation data setting the fragmentor voltage at 200 V in a CE-ESI(+)-TOF-MS system for 17 modified L-amino acid authentic standards. AAs were divided into five groups according to the typical fragments ions generated from AAH^+ based on their molecule-specific fragmentation behaviors and according to the reactivity of their side chain.

Table S3. Fragments results for 18 related compounds.

Compound Name	Molecular formula	Monoisotopic mass	RMT	$[M+H]^+$	Fragments to 200 V
Related-AAs GROUP 1.					
DL-norvaline	$C_5H_{11}NO_2$	117.0790	0.86	118.086	55.0542, **72.0808**
L-norleucine	$C_6H_{13}NO_2$	131.0946	0.91	132.1019	69.0707, **86.0972**
Related-AAs GROUP 2.					
kynurenic acid	$C_{10}H_7NO_3$	189.0426	1.99	190.0498	63.0243, 89.0402, 116.0511, **144.0463**, 172.0402, 174.0551
L -pyroglutamic acid	$C_5H_7NO_3$	129.0426	1.75	130.0499	**84.0451**, 102.0556
L-ornithine	$C_5H_{12}N_2O_2$	132.0899	0.61	133.0966	**70.0661**, 87.0917, 115.0866, 116.0707
L-picolinic acid	$C_6H_5NO_2$	123.0320	1.39	124.0391	**78.0349,** 106.0291
Related-AAs GROUP 3.					
DL-homocysteine	$C_4H_9NO_2S$	135.0354	0.89	136.0427	56.0561, 73.0111, **90.0377**, 118.0322
DL-homocystine	$C_8H_{16}N_2O_4S_2$	268.0551	0.84	269.0624	**88.0222**, 90.0376, 102.0550, 134.0271, 136.0426
Related-AAs GROUP 4.					
L-homoserine	$C_4H_9NO_3$	119.0582	0.86	120.066	56.0495, 74.0241, **74.0600**, 84.0448, 102.0550
Related-AAs GROUP 5.					
L-homoarginine	$C_7H_{16}N_4O_2$	188.1290	0.70	**189.1374**	60.0563, 84.0813, 99.0917, 102.0918, 126.1040, 130.0860, 144.1137, 147.1128, 171.1240, 172.1080
Others					
creatinine	$C_4N_3H_7O$	113.0589	0.73	114.0666	**72.0451**
taurine	$C_2H_7NO_3S$	125.0147	1.56	126.0214	78.9847, **108.0109**
L-pipecolic acid	$C_6H_{11}NO_2$	129.0790	0.87	130.0863	56.0504, **84.0813**, 112.0760
creatine	$C_4H_9N_3O_2$	131.0695	0.83	132.0768	69.0455, 87.0563, **90.0554,** 114.0663, 115.0513
DL-5-hydroxy-L-lysine	$C_6H_{14}N_2O$	162.1004	0.65	163.1080	55.0550, 74.0241, **82.0657**, 84.0813, 99.0917, 100.0760, 110.0633, 116.0705, 118.0860, 127.0864, **128.0710**, 145.0970, 146.0810
L-methionine sulfoxide	$C_5H_{11}NO_3S$	165.0460	0.99	166.0537	56.0489, **74.0243**, 84.0457, 102.0552, 131.0160, 146.0163, 149.0264
DL-citrulline	$C_6H_{13}N_3O_3$	175.0957	0.95	176.1019	**70.0660**, 113.0706, 115.0870, 116.0715, 130.0929, 133.1008, 141.0646, 159.0757
***O*-phospho-L-serine**	$C_3H_8NO_6P$	185.0089	2.02	186.0162	**88.0396**, 136.9309

m/z values for the **diagnostic ion** are given in bold type.

Table S3. Compilation of all fragmentation data setting the fragmentor voltage at 200 V in a CE-ESI(+)-TOF-MS system for 18 related L-amino acids authentic standards. AAs were divided into five groups according to the typical fragments ions generated from AAH^+ based on their molecule-specific fragmentation behaviors and according to the reactivity of their side chain.

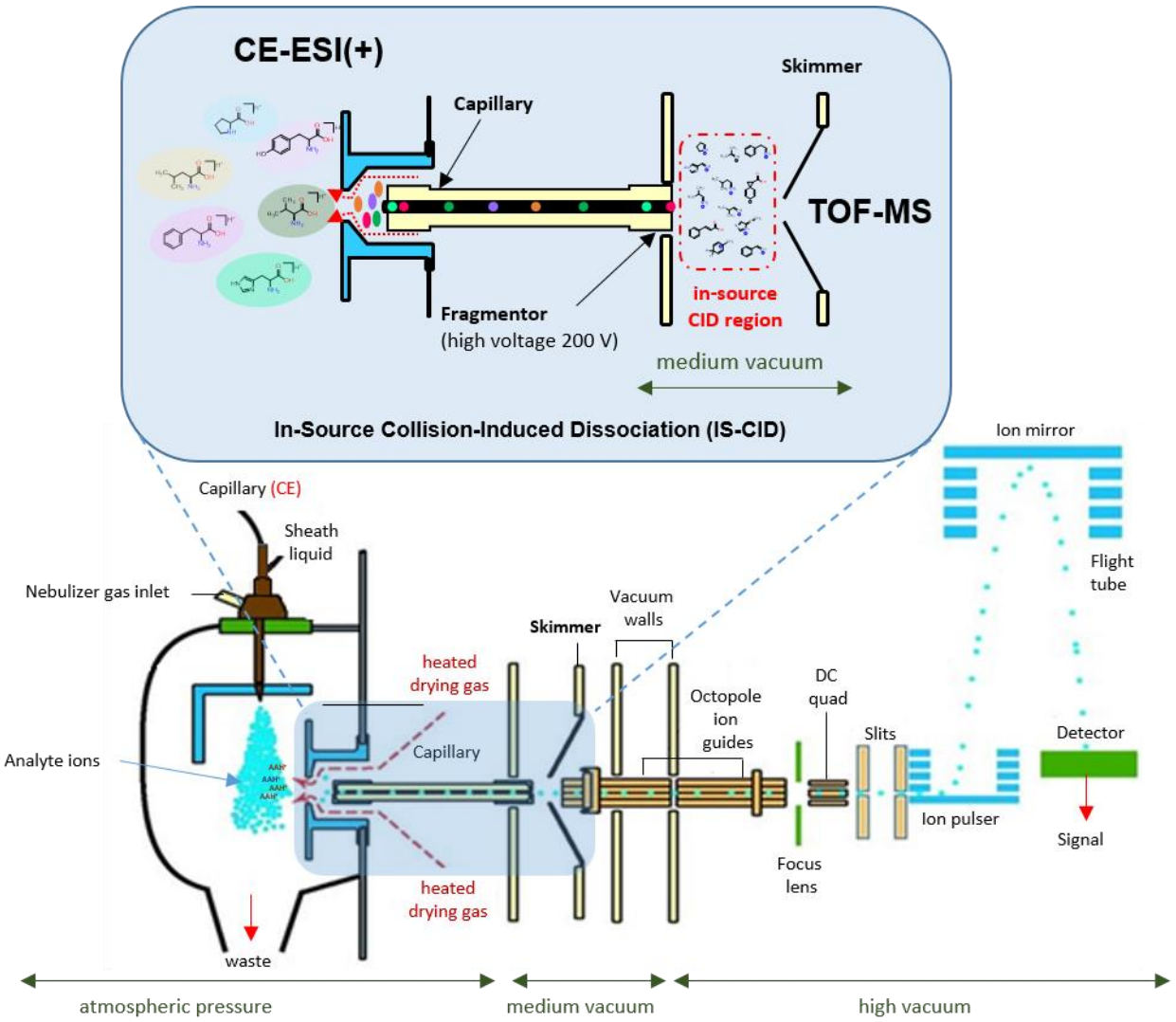

Figure S1. Schematic of the in-source CID region in a CE-ESI(+)-TOF-MS system (image courtesy of Agilent). The fragmentor voltage represents the voltage between the outlet of the capillary and the skimmer at the entrance to the mass analyzer. Formation of ions in the transition region between the ESI source and the ion optics of a mass analyzer at relatively high pressures, compared to the low pressure normally observed in collision chambers.

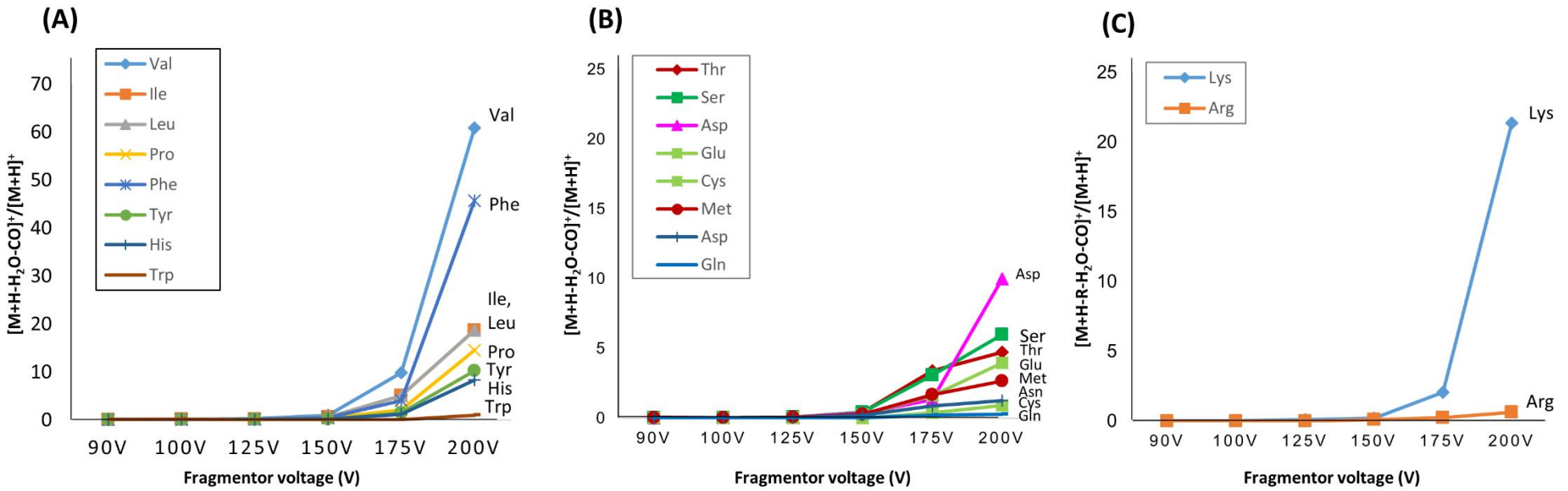

Figure S2. Variations in the fragmentor voltage for characterisitic ions generation. (A) Variations in the ion intensity ratio of $[M+H-H_2O-CO]^+/[M+H]^+$ for AAs from Groups 1 and 2 (aliphatic and aromatic AAs respectively) with the fragmentor voltage. The relative abundances of the immonium ion increased by an enhacement of the fragmentor voltage. (B) Variations in the ion intensity ratio of $[M+H-H_2O-CO]^+/[M+H]^+$ for AAs from Groups 3 and 4 with the fragmentor voltage. The relative abundances of the immonium ion increased by an enhacement of the fragmentor voltage. (C) Variations in the ion intensity ratio of $[M+H-R-H_2O-CO]^+/[M+H]^+$ for AAs from Group 5 with the fragmentor voltage. The relative abundances of the diagnostic ion increased by an enhacement of the fragmentor voltage. R = NH_2 for L-Lys and R = guanidine for L-Arg.

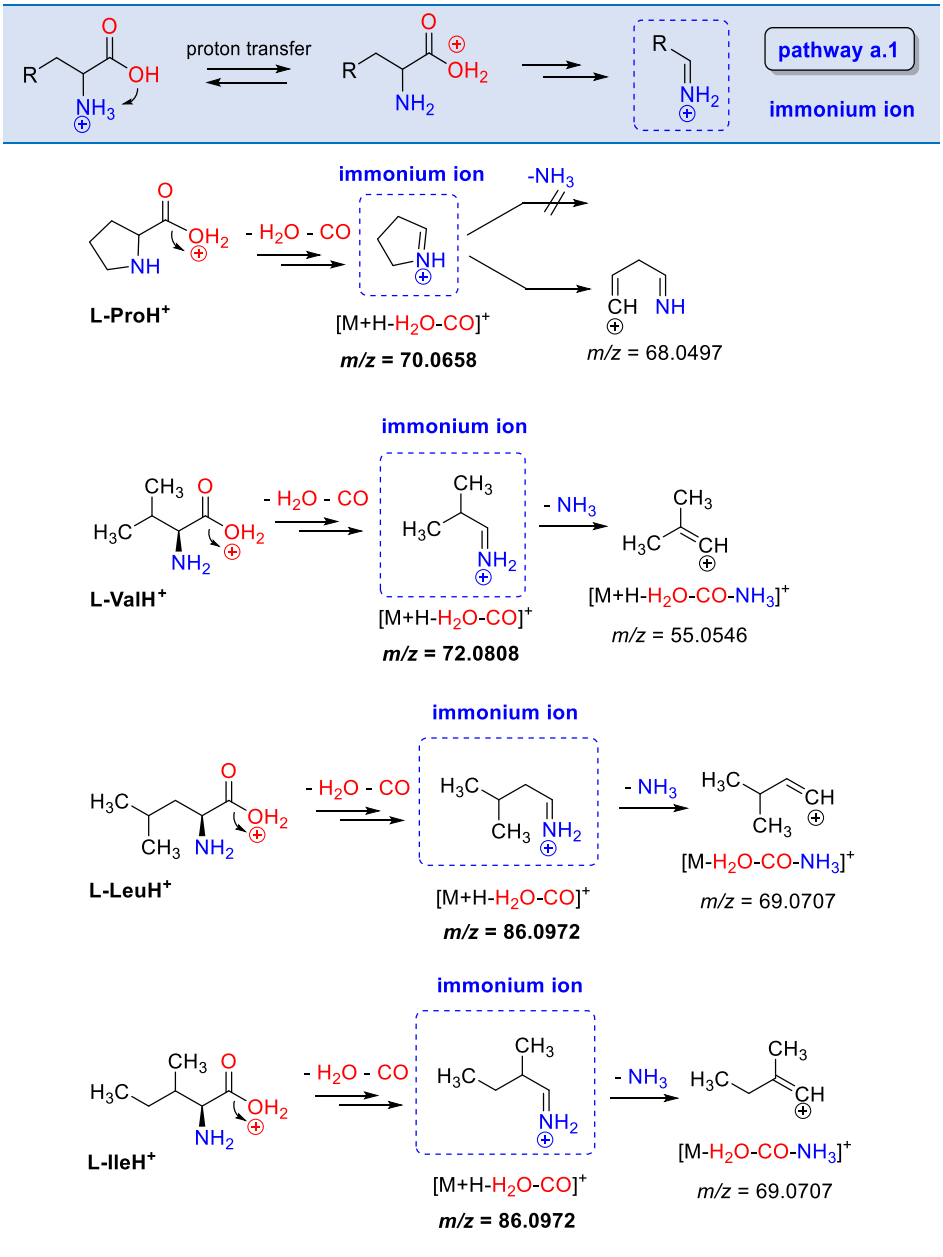

Figure S3. Fragmentation mechanisms for structural assignment of the diagnostic ions from aliphatic amino acids (Group 1). Protonated AAs containing alkyl group in the side-chain (**L-ValH$^+$**, **L-LeuH$^+$**, **L-IleH$^+$**) fragment primarily by elimination of (H_2O+CO) from the carbohydroxy head group yielding the characteristic immonium ion fragment, as a base peak, followed by elimination of ammonia and yielding the fragment $[M+H-H_2O-CO-NH_3]^+$ following Pathway a.1, except the cycloalkyl (**L-ProH$^+$**).

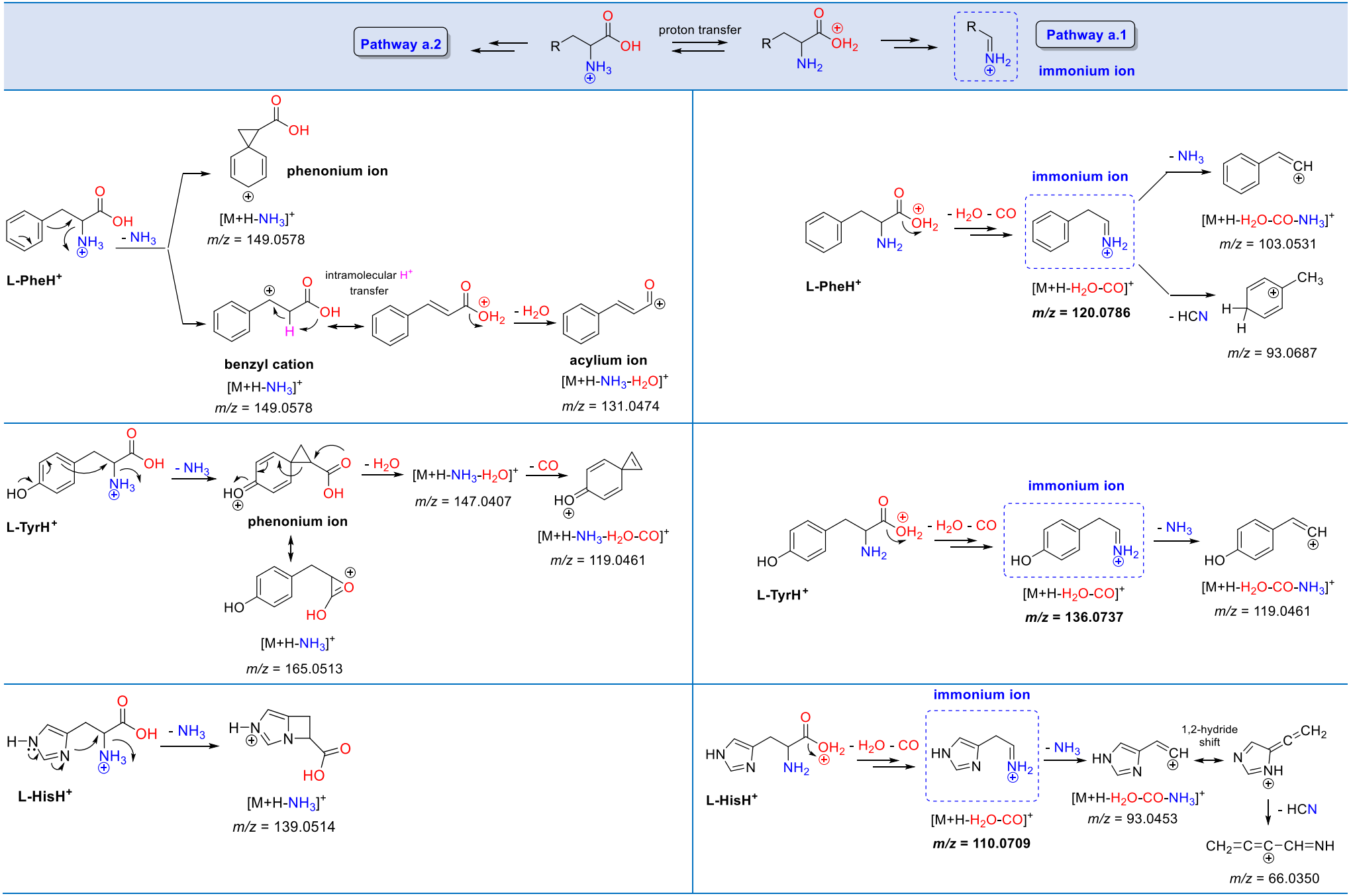
Pathway a.2
proton transfer
Pathway a.1
immonium ion
phenonium ion
[M+H-NH3]+
m/z = 149.0578
- NH3
L-PheH+
intramolecular H+ transfer
benzyl cation
[M+H-NH3]+
m/z = 149.0578
- H2O
acylium ion
[M+H-NH3-H2O]+
m/z = 131.0474
- H2O - CO
immonium ion
[M+H-H2O-CO]+
m/z = 120.0786
- NH3
[M+H-H2O-CO-NH3]+
m/z = 103.0531
- HCN
m/z = 93.0687
L-TyrH+
- NH3
phenonium ion
[M+H-NH3-H2O]+
m/z = 147.0407
- H2O
- CO
[M+H-NH3-H2O-CO]+
m/z = 119.0461
[M+H-NH3]+
m/z = 165.0513
- H2O - CO
immonium ion
[M+H-H2O-CO]+
m/z = 136.0737
- NH3
[M+H-H2O-CO-NH3]+
m/z = 119.0461
L-HisH+
- NH3
[M+H-NH3]+
m/z = 139.0514
- H2O - CO
immonium ion
[M+H-H2O-CO]+
m/z = 110.0709
- NH3
[M+H-H2O-CO-NH3]+
m/z = 93.0453
1,2-hydride shift
- HCN
CH2=C=C-CH=NH
m/z = 66.0350

Figure S4. Fragmentation mechanisms for structural assignment of the diagnostic ions from aromatic amino acids (Group 2). Protonated AAs containing aromatic groups (**L-HisH$^+$, L-PheH$^+$, L-TyrH$^+$, L-TrpH$^+$**) exhibit a competition between the most favored immonium ion as a base peak, Pathway a.1., with the ammonia-loss, Pathway a.2., fragment $[M+H-NH_3]^+$, which is initiated from nucleophilic attack of the aromatic ring on the side chain to carbonyl carbon which initiates the elimination of NH_3, common to all aromatic AAs. Harrison's group has proposed, in a detailed study of the low-energy fragmentation reaction for AAH^+, a mechanism for the loss of NH_3 from L-PheH$^+$, L-TyrH$^+$ in which the aromatic group migrates to form the phenonium ion with concomitant elimination of NH_3.[12] This same mechanism was supported by Rogalewicz *et al*. who emphasized the electron-donating property of the phenolic OH in stabilizing the phenonium ion.[13] [14] In addition, Shoeib *et al*. for L-PheH$^+$ proposed an alternative mechanism for the elimination of NH_3 involving a benzyl cation. The ions initially formed by loss of NH_3 are phenonium ions, but subsequent fragmentation is most easily understood in terms of the isomeric benzyl cation structures. [8]

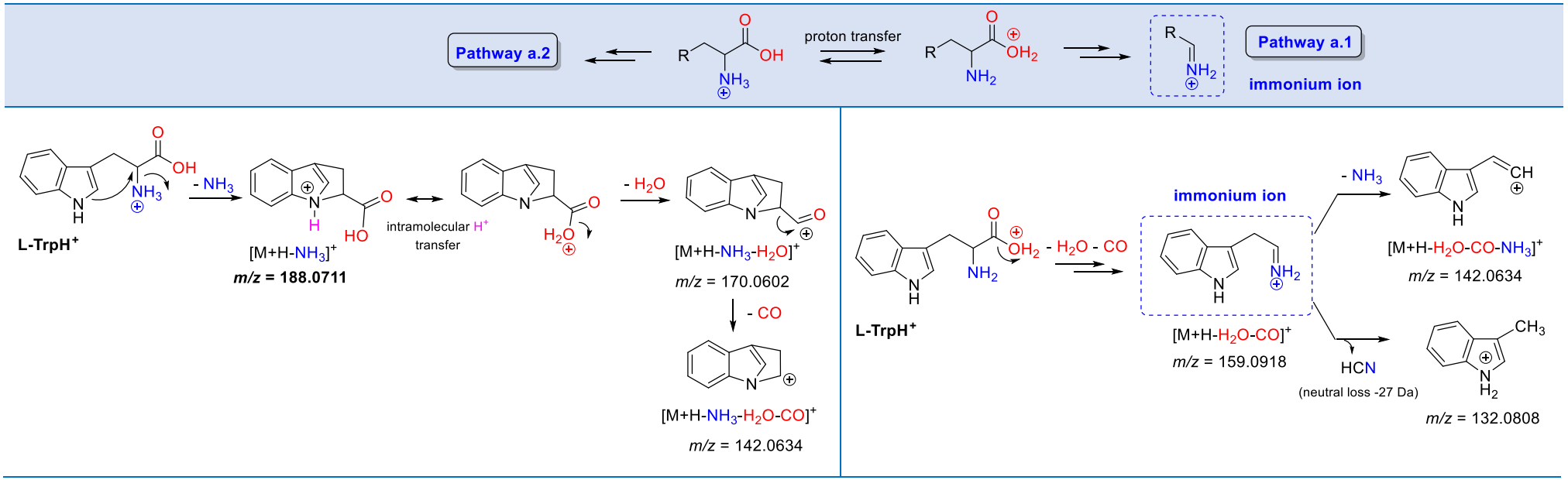

Figure S4 cont. Fragmentation mechanisms for structural assignment of the diagnostic ions from TrpH$^+$ (Group 2). L-TrpH$^+$ exhibits facile loss of NH_3, helped by the assistance of the aromatic group, to yield fragment $[M+H-NH_3]^+$ as a base peak coming from the prominent Pathway a.2. [15]

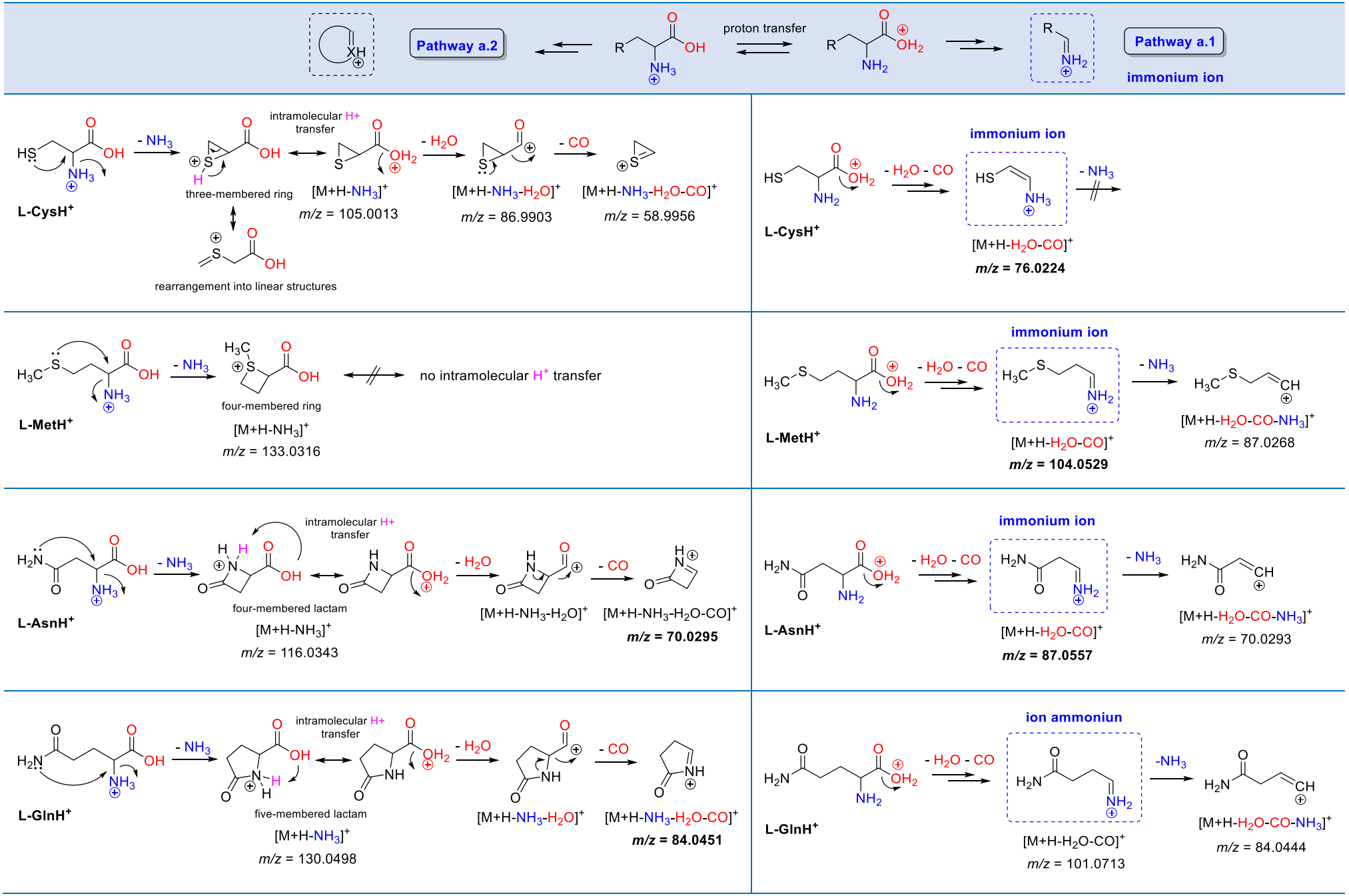
Pathway a.2
proton transfer
Pathway a.1
immonium ion
- NH3
intramolecular H+ transfer
- H2O
- CO
three-membered ring
rearrangement into linear structures
L-CysH+
[M+H-NH3]+
m/z = 105.0013
[M+H-NH3-H2O]+
m/z = 86.9903
[M+H-NH3-H2O-CO]+
m/z = 58.9956
immonium ion
- H2O - CO
- NH3
[M+H-H2O-CO]+
m/z = 76.0224
L-MetH+
four-membered ring
[M+H-NH3]+
m/z = 133.0316
no intramolecular H+ transfer
[M+H-H2O-CO]+
m/z = 104.0529
[M+H-H2O-CO-NH3]+
m/z = 87.0268
L-AsnH+
four-membered lactam
m/z = 116.0343
[M+H-NH3-H2O]+
[M+H-NH3-H2O-CO]+
m/z = 70.0295
m/z = 87.0557
m/z = 70.0293
L-GlnH+
five-membered lactam
m/z = 130.0498
m/z = 84.0451
ion ammoniun
-NH3
m/z = 101.0713
m/z = 84.0444

Figure S5. Fragmentation mechanisms for structural assignment of the diagnostic ions from sulfur-containing and amidic amino acids (Group 3). Protonated AAs containing a sulfur-containing (L-MetH^+, L-CysH^+) and an amidic group on the side-chain (L-AsnH^+, L-GlnH^+) show NH_3 lost by direct cleavage assisted by the side-chain. The favored ammonia-loss pathway, fragment $[M+H-NH_3]^+$, is due to an a rearrangement between the side-chain group and the protonated α-amino group. A nucleophilic attack from the backbone (S or N) on the side chain to Cα to the carboxyl group initiates the elimination of α-NH_3 and the formation of three-, four- and five-membered intermediate ring structures. An intramolecular H^+ transfer is involved in the further loss of H_2O from the α-carbohydroxy group, accompanied by loss of CO. Compounds that showed equal competitive fragmentation pathways never showed significant intensity in the diagnostic ion (Supporting Spectra group 3).

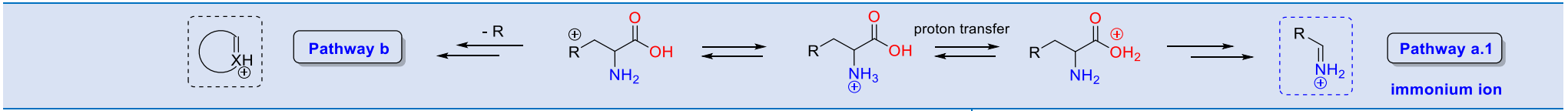
Pathway b
- R
proton transfer
Pathway a.1
immonium ion

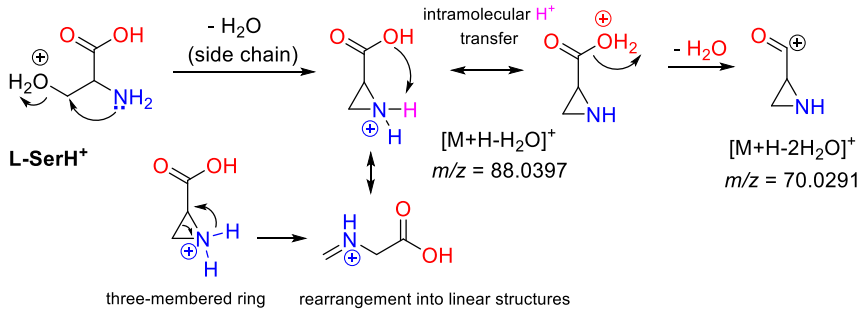
- H2O
(side chain)
intramolecular H+
transfer
- H2O
L-SerH+
[M+H-H2O]+
m/z = 88.0397
[M+H-2H2O]+
m/z = 70.0291
three-membered ring
rearrangement into linear structures

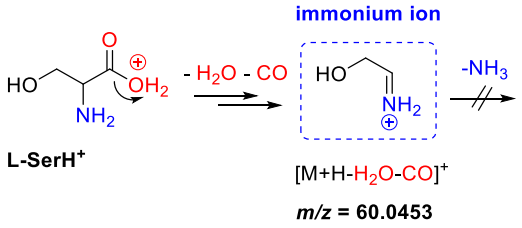
immonium ion
- H2O - CO
-NH3
L-SerH+
[M+H-H2O-CO]+
m/z = 60.0453

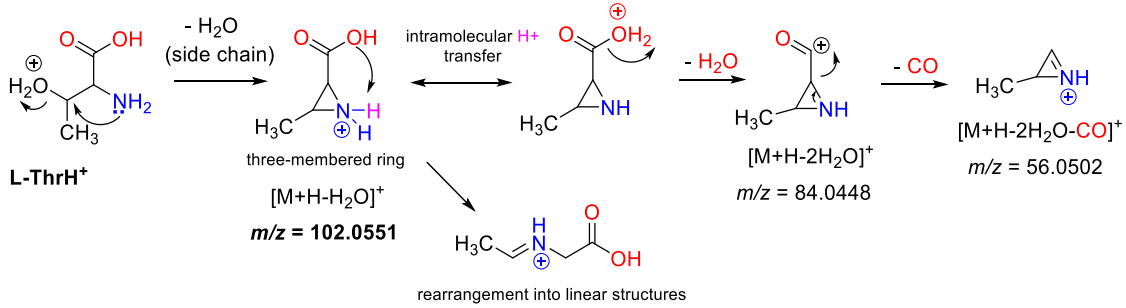
- H2O
(side chain)
intramolecular H+
transfer
- H2O
- CO
L-ThrH+
three-membered ring
[M+H-H2O]+
m/z = 102.0551
[M+H-2H2O]+
m/z = 84.0448
[M+H-2H2O-CO]+
m/z = 56.0502
rearrangement into linear structures

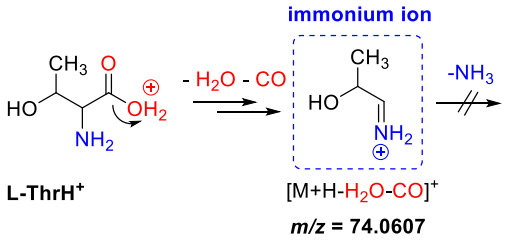
immonium ion
- H2O - CO
-NH3
L-ThrH+
[M+H-H2O-CO]+
m/z = 74.0607

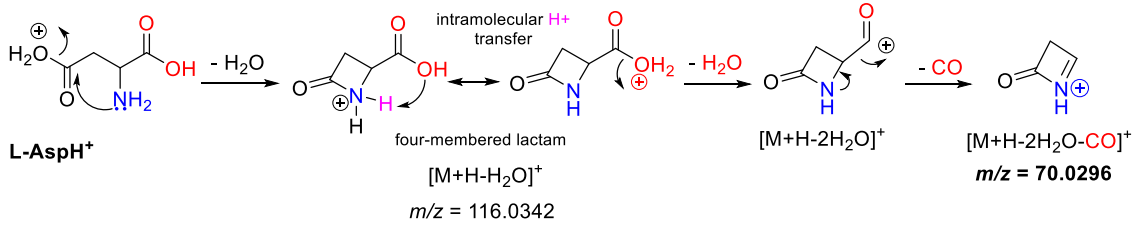
- H2O
intramolecular H+
transfer
- H2O
- CO
L-AspH+
four-membered lactam
[M+H-H2O]+
m/z = 116.0342
[M+H-2H2O]+
[M+H-2H2O-CO]+
m/z = 70.0296

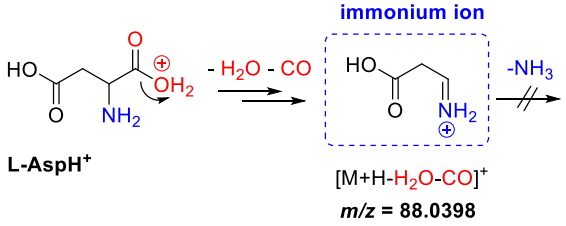
immonium ion
- H2O - CO
-NH3
L-AspH+
[M+H-H2O-CO]+
m/z = 88.0398

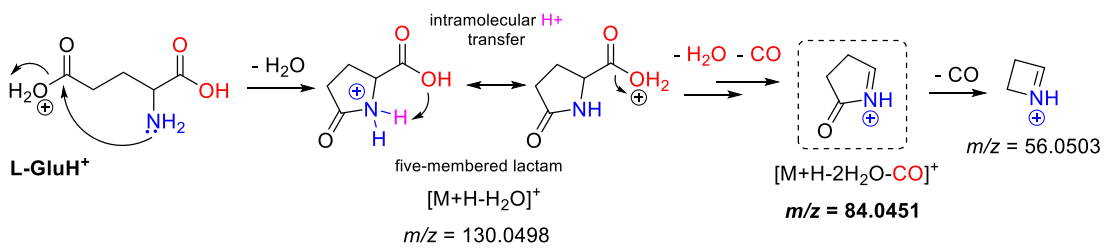
- H2O
intramolecular H+
transfer
- H2O - CO
- CO
L-GluH+
five-membered lactam
[M+H-H2O]+
m/z = 130.0498
[M+H-2H2O-CO]+
m/z = 84.0451
m/z = 56.0503

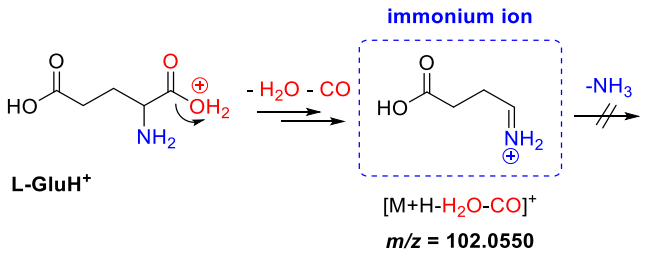
immonium ion
- H2O - CO
-NH3
L-GluH+
[M+H-H2O-CO]+
m/z = 102.0550

Figure S6. Fragmentation mechanisms for structural assignment of the diagnostic ions from hydroxilic and acidic amino acids (Group 4). Protonated AAs containing hydroxylic (L-SerH$^+$, L-ThrH$^+$) and acidic (L-AspH$^+$, L-GluH$^+$) group in the side-chain fragmented primarily by elimination of (H_2O+CO) from the carbohydroxy head group yielding the characteristic **immonium ion** as a base peak, Pathway a.1. Not elimination of NH_3 was observed, instead, fragment *elimination* of H_2O from the hydroxylic oxygen of the side-chain, followed by the loss of (H_2O+CO) was observed, Pathway b. These fragment ions abundances, Table 1, were determined by a competition between immonium ion generation and water-loss pathways. Compounds that showed equal competitive fragmentation pathways never showed significant intensity in the diagnostic ion (Supporting Spectra group 4). The formation mechanism of $[M+H-H_2O]^+$ from $[M+H]^+$ was due to an a rearrangement between the α-amino group and the protonated side-chain group. The structures of $[M+H-H_2O]^+$ were a three, four, and five-membered ring structures respectively. Only the three-membered rings could be rearranged into linear structures, whereas the four- and five-membered ring might not be rearranged into a linear one.[9]

L-lysine

Pathway a.2.

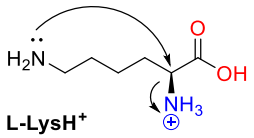

Pathway b.

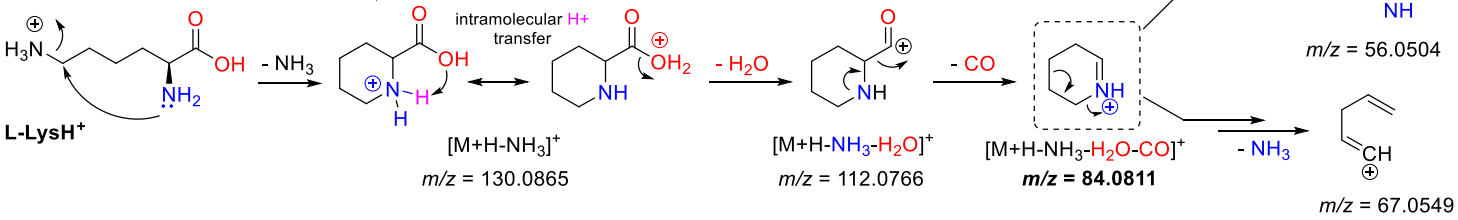

L-arginine

Pathway a.2.

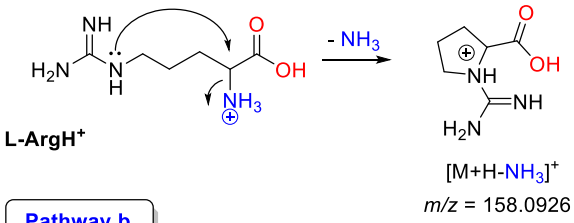

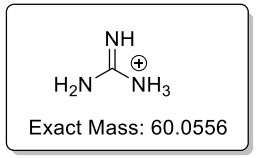

Pathway b.

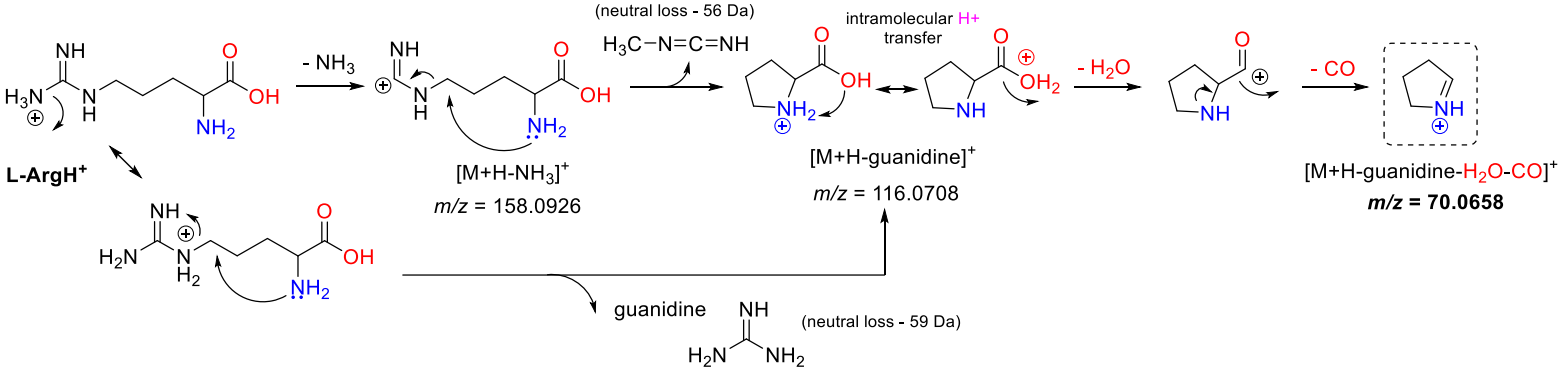

Figure S7. Major Fragmentation pathways for structural assignment of the diagnostic ions from basic amino acids (Group 5). Protonated AAs containing basic group in the side-chain (L-LysH^+, L-ArgH^+), show loss of NH_3 from the side-chain as Harrison's studies[12] have demonstrated on the fragmentation chemistry of L-LysH^+. L-ArgH^+ shows a variety of fragmentation pathways, including loss of NH_3, amidine or guanidine from the protonated side-chain group by α-amino group assistance to form fragment $[M+H-NH_3]^+$. Such competition and the differences in the intensity of the main characteristic ions observed were due in the formation of charged species.

Modified L-lysine derivatives

Pathway a.2.

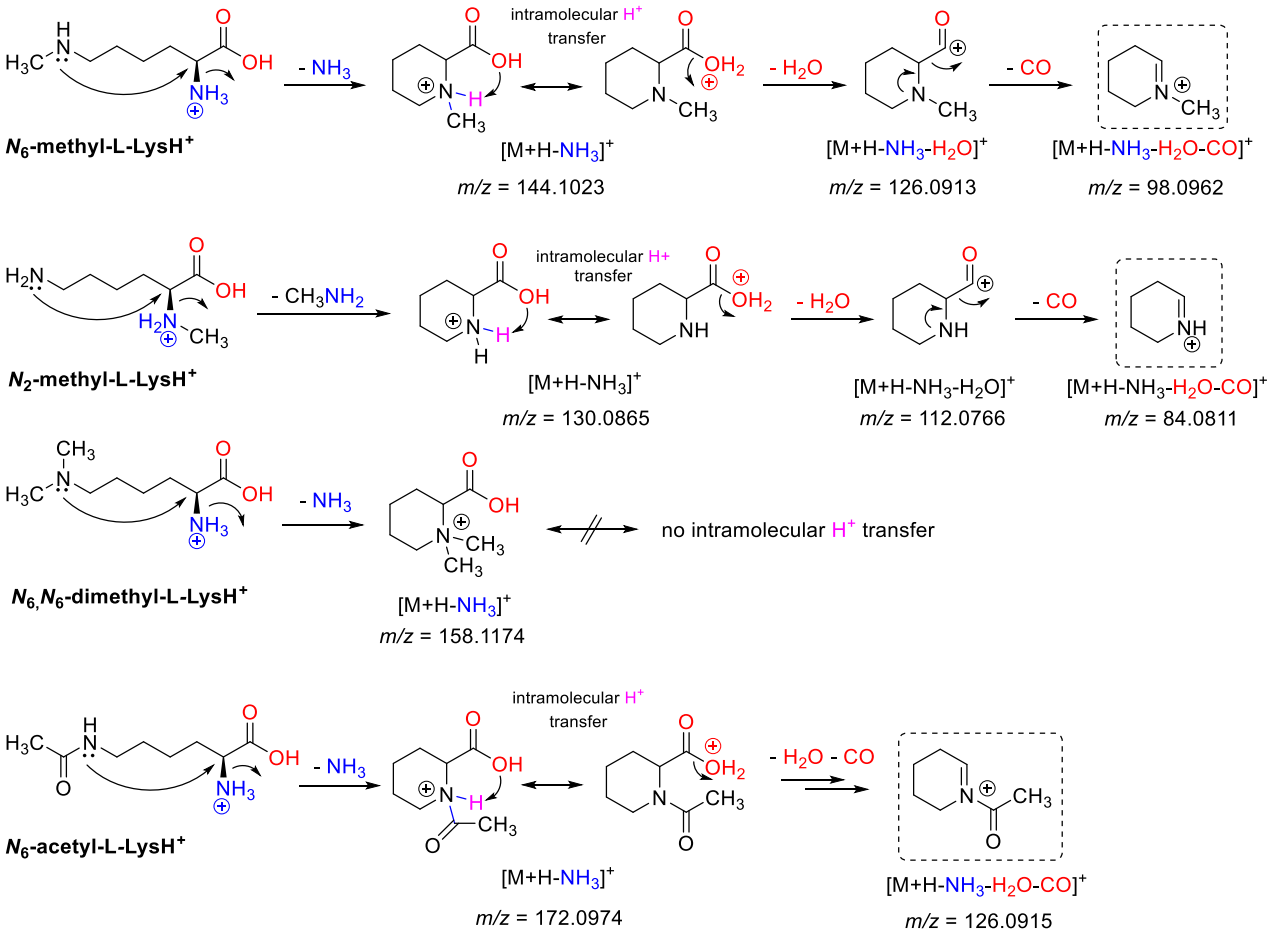

Pathway b.

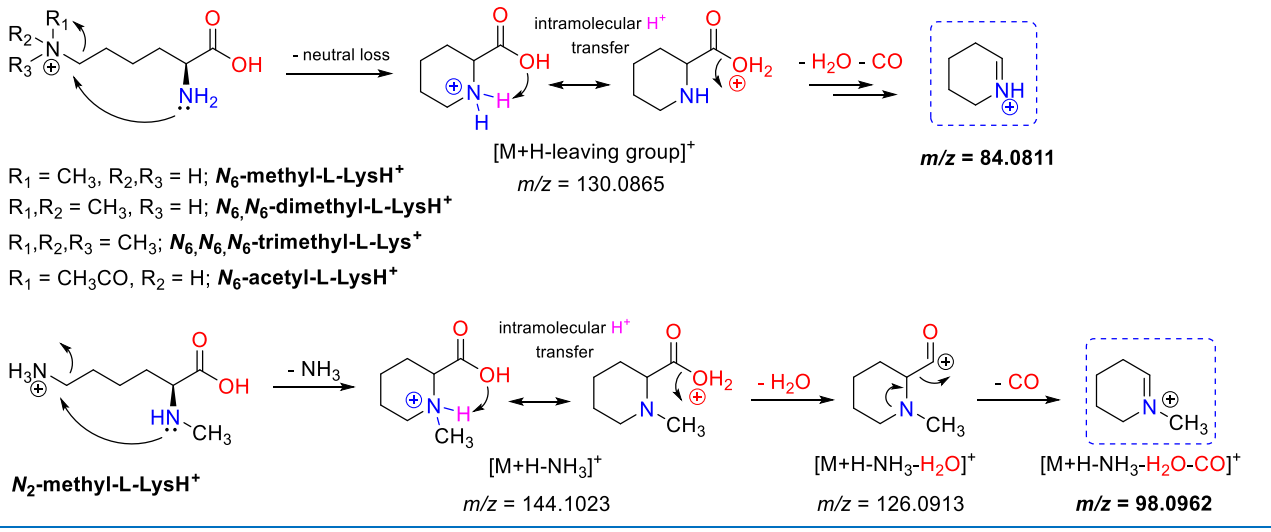

Figure S8. Proposed competition fragmentation pathways for modified L-LysH$^+$ derivatives.

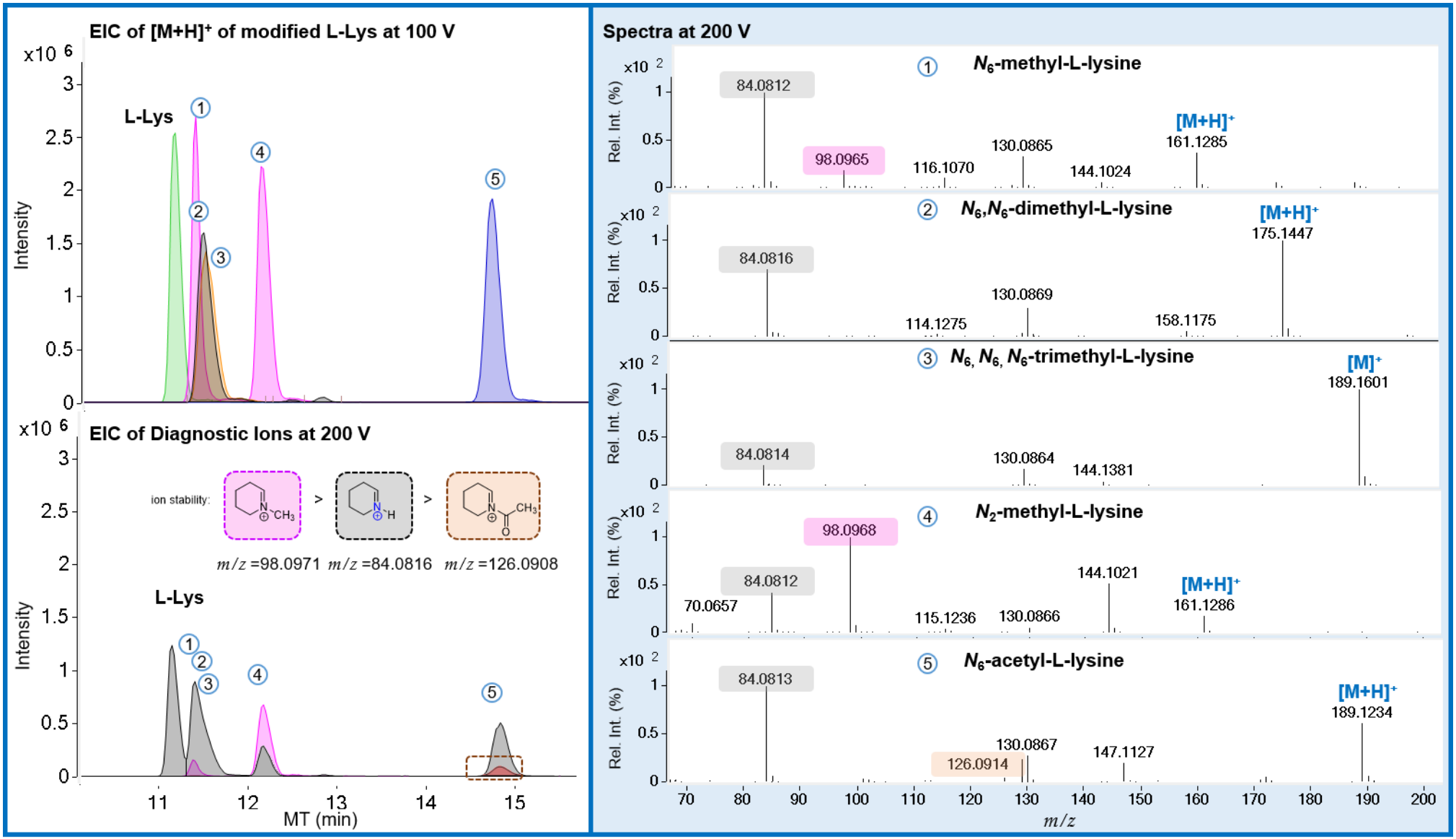

Figure S9. Standard mixture containing modified L-Lys derivatives at the same concentration analyzed under CE-ESI(+)-TOF-MS optimized conditions.

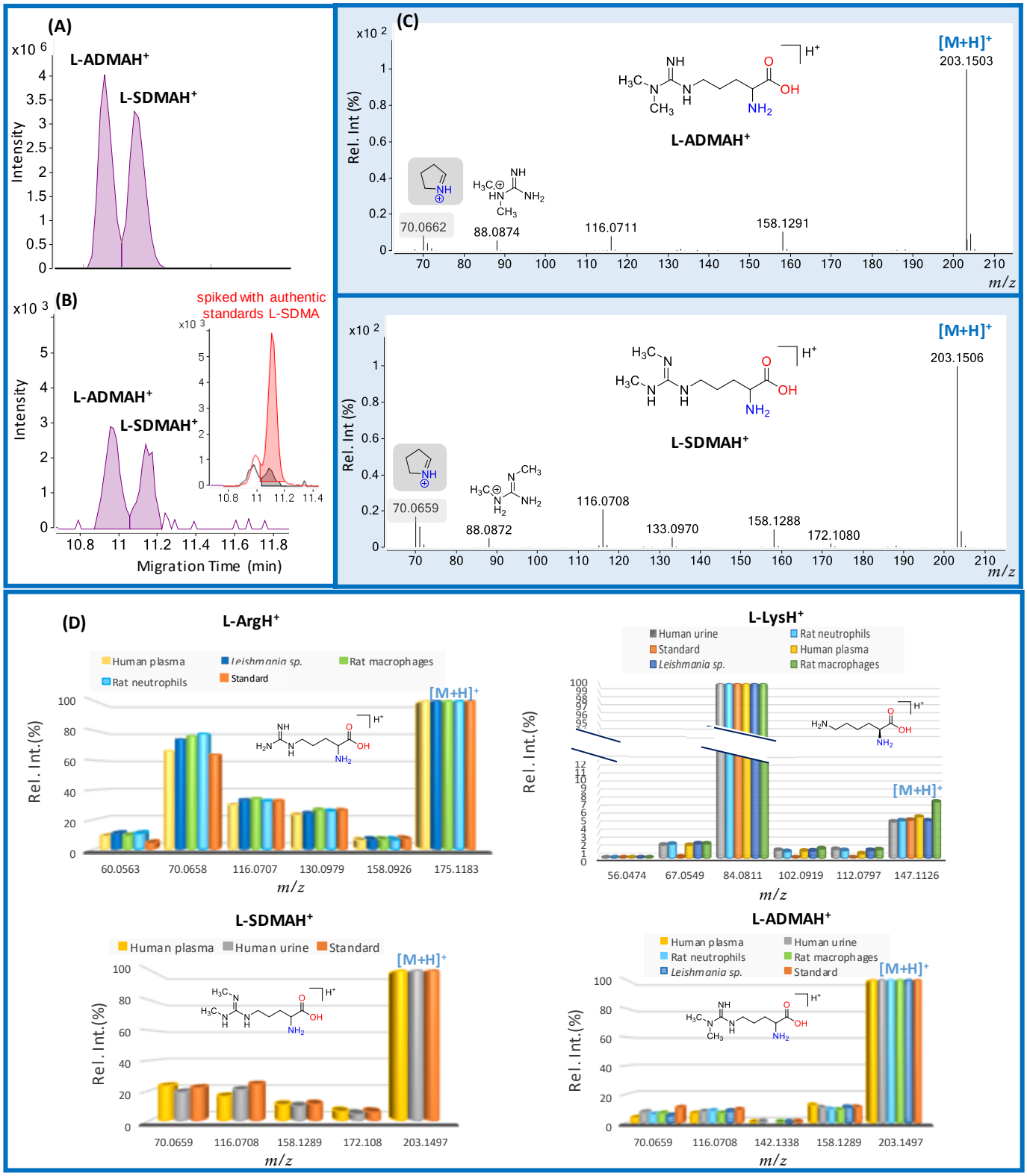

Figure S10. Standard mixture containing two modified L-Arg derivatives at the same concentration analyzed under CE-ESI(+)-TOF-MS optimized conditions. (A) Extracted Ion Chromatograms (EIC) for m/z =70.0658 setting the fragmentor voltage at 200 V for L-SDMA and L-ADMA in the authentic standard mixture. (B) Extracted Ion Chromatograms (EIC) for m/z = 70.0658 setting the fragmentor voltage at 200 V for L-SDMA and L-ADMA in human plasma. Authentic standards, L-ADMA and L-SDMA, were spiked into human plasma samples to definitively identify them. (C) In-source mass spectra for studied compounds. (D) Fragmentation behavior in complex biological samples. The most intense ion is assigned an abundance of 100%, and it is referred to as the base peak. The graphic shows % of relative abundance of major ions present in modified L-ArgH$^+$ derivatives spectra. L-Arg commercial standard was used always as references for matrix evaluation on fragmentation behavior.

Symmetric N_G,N_G-dimethyl-L-arginine (L-SDMA)

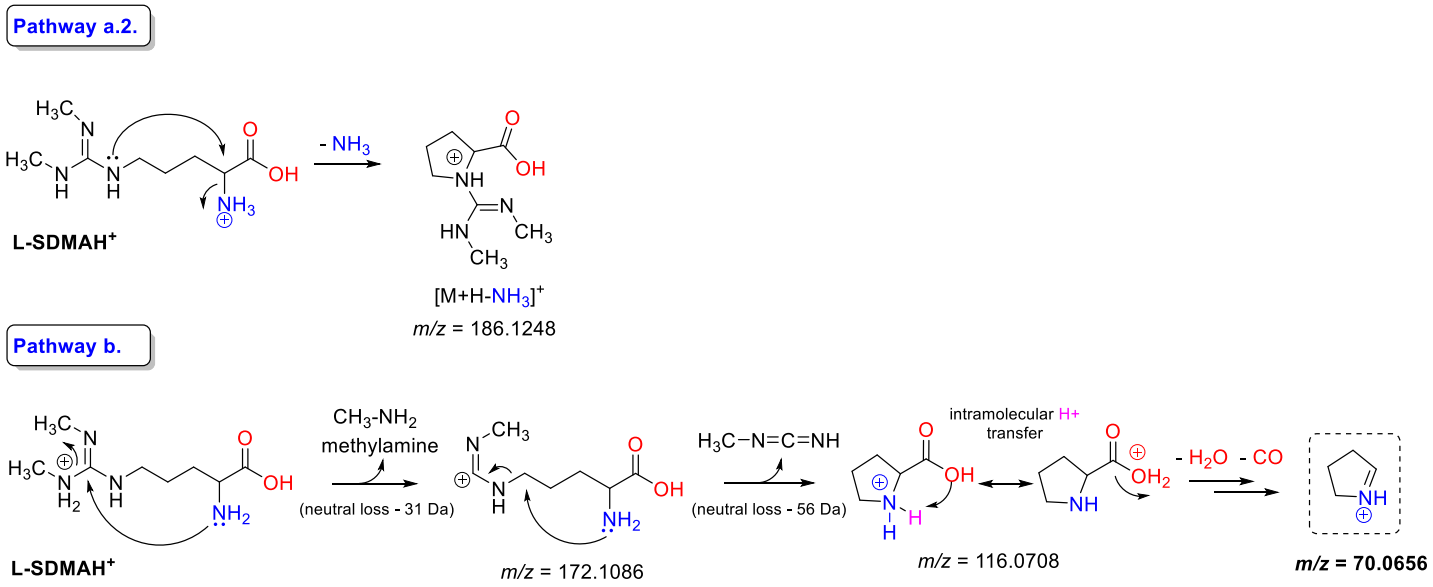

Asymmetric N_G,N_G-dimethyl-L-arginine (L-ADMA)

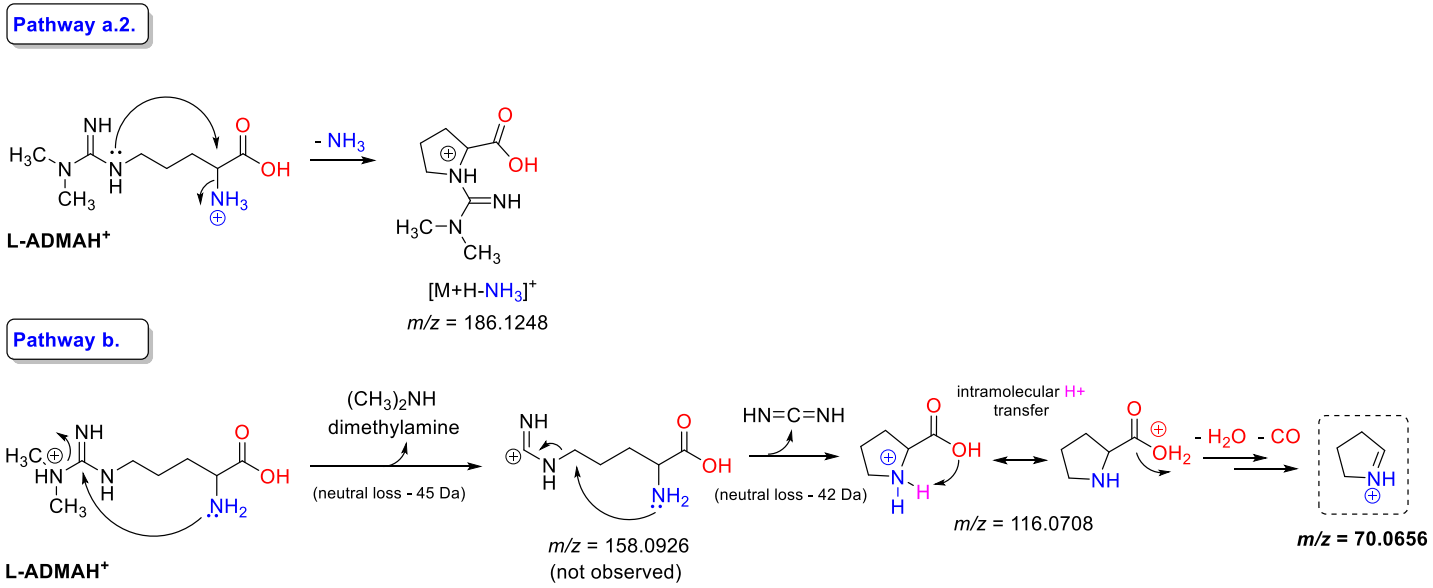

Figure S11. Proposed mayor fragmentation pathway for the protonated *N,N*-dimethyl-L-ArgH$^+$ derivatives.

Modified L-Arginine derivatives

Pathway c.

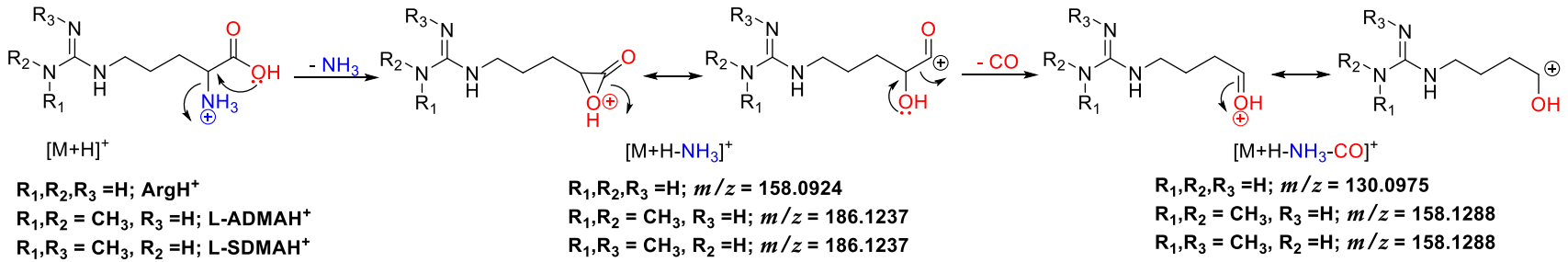

R_1,R_2,R_3 =H; ArgH$^+$
R_1,R_2 = CH_3, R_3 =H; L-ADMAH$^+$
R_1,R_3 = CH_3, R_2 =H; L-SDMAH$^+$

R_1,R_2,R_3 =H; m/z = 158.0924
R_1,R_2 = CH_3, R_3 =H; m/z = 186.1237
R_1,R_3 = CH_3, R_2 =H; m/z = 186.1237

R_1,R_2,R_3 =H; m/z = 130.0975
R_1,R_2 = CH_3, R_3 =H; m/z = 158.1288
R_1,R_3 = CH_3, R_2 =H; m/z = 158.1288

Figure S11 cont. Unusual fragmentation pathway for the protonated *N*,*N*-dimethyl-L-ArgH$^+$ derivatives, Pathway a.3.

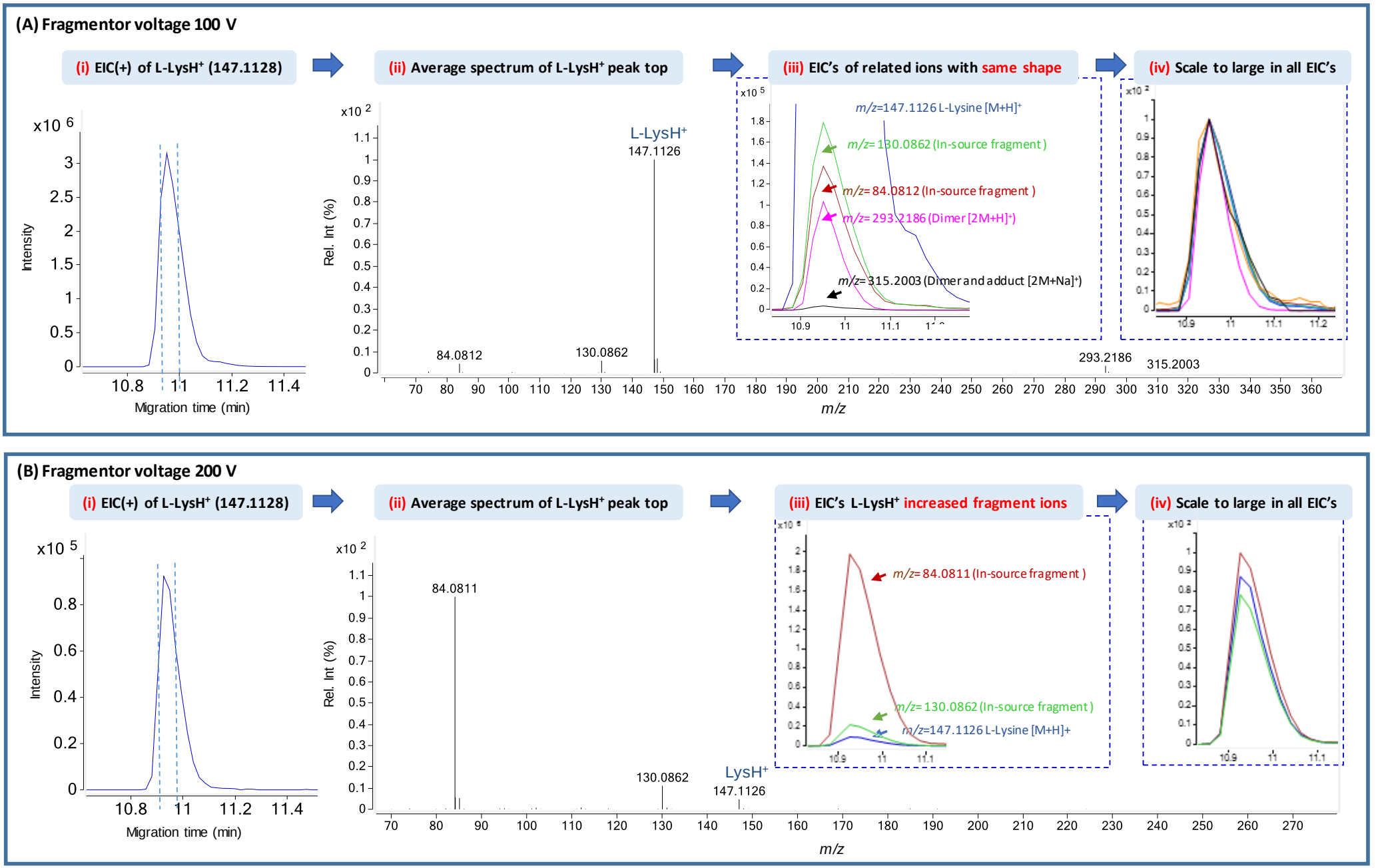
(A) Fragmentor voltage 100 V
(i) EIC(+) of L-LysH+ (147.1128)
(ii) Average spectrum of L-LysH+ peak top
(iii) EIC's of related ions with same shape
(iv) Scale to large in all EIC's
Intensity
Migration time (min)
Rel. Int (%)
L-LysH+
147.1126
84.0812
130.0862
293.2186
315.2003
m/z
m/z=147.1126 L-Lysine [M+H]+
m/z= 130.0862 (In-source fragment)
m/z= 84.0812 (In-source fragment)
m/z= 293.2186 (Dimer [2M+H]+)
m/z=315.2003 (Dimer and adduct [2M+Na]+)
(B) Fragmentor voltage 200 V
(i) EIC(+) of L-LysH+ (147.1128)
(ii) Average spectrum of L-LysH+ peak top
(iii) EIC's L-LysH+ increased fragment ions
(iv) Scale to large in all EIC's
Intensity
Migration time (min)
Rel. Int (%)
84.0811
130.0862
LysH+
147.1126
m/z
m/z= 84.0811 (In-source fragment)
m/z= 130.0862 (In-source fragment)
m/z=147.1126 L-Lysine [M+H]+

Figure S12. Strategy for the peak identification of L-lysine as an example. (A) First, at 100 V, extract the Extracted Ion Chromatogram (EIC) for m/z =147.1128; secondly, extract the spectrum of the top of the peak. Third, extract the EIC of all m/z observed in the spectrum that correspond to fragments and adducts. Finally, peak grouping: every m/z belonging to the same compound must have the same peak shape as the corresponding $[M+H]^+$. (B) The same steps as above are followed for 200 V. In the third step, the increase of the intensity of the fragments and the decrease of the intensity of the $[M+H]^+$ are observed.

Case Study 1. Targeted screening analysis of *N*-methyl-L-lysines in human plasma

Step 1

Human plasma sample analyzed at 100 V and 200 V
Molecular Feature after deconvolution

Matching against CEU Mass Mediator, considering exp. **RMT** and **$[M+H]^+$** ***m/z*** **161.1286,** candidate:
- ***N_6*-methyl-L-lysine (MAA)**

Adding ***N_2*-methyl-L-lysine** to candidate list due to structural similarity

Targeted screening of **diagnostic ion (DI)** ***m/z*** **84.0811** at 200 V

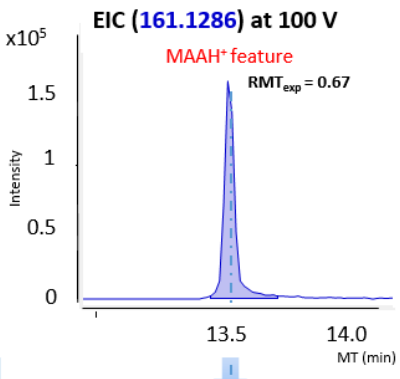

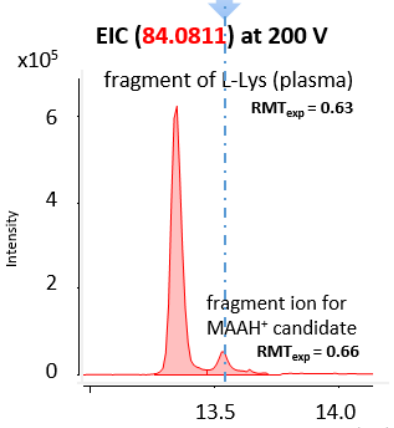

Step 2

Extracting experimental IS-CID spectrum for $MAAH^+$ candidate at 200 V

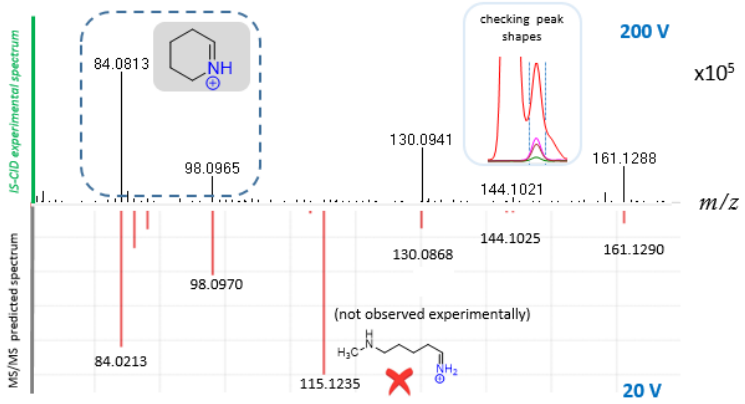

Comparison with the ISF MS spectra of authentic standards

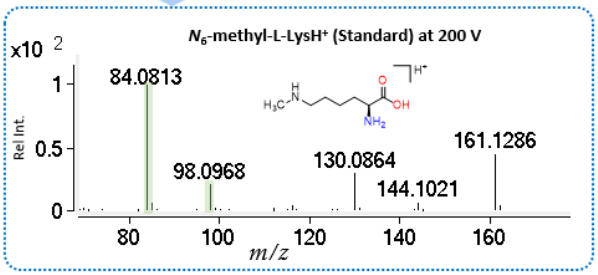

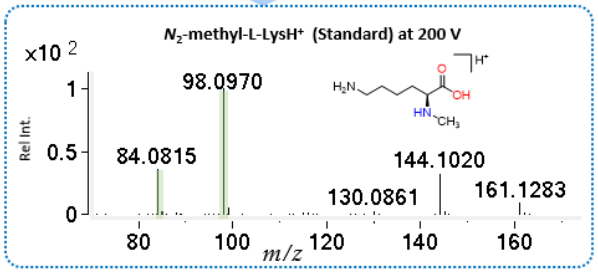

Step 4

Validation: Spiking sample with authentic standards; N_6-methyl and N_2-methyl-L-Lysine

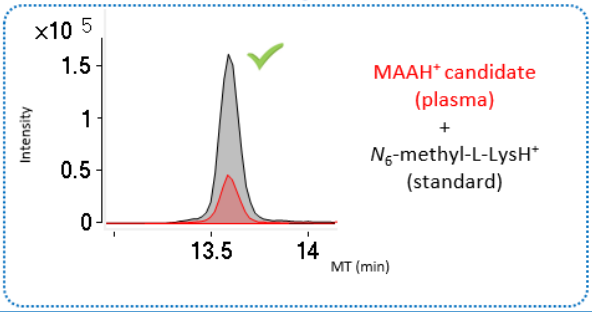

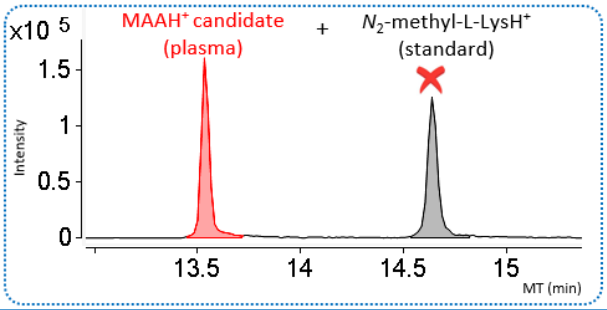

Figure S13. Case Study 1: Targeted screening analysis of *N*-methyl-L-lysines in human plasma sample. Step1, Spectral deconvolution for the sample measured at 100 V with MassHunter Profinder software version B.08.00 (Agilent Technologies, Santa Clara, CA, USA). Then, Extracted Ion Chromatogram (EIC) for m/z 161.1286 at 100 V with MassHunter Qualitative Analysis Software version B.08.00 (Agilent Technologies). Matching with CMM and databases for a list of putative candidates. Based on DI as base peak, N_6-methyl-L-Lys was ranked as the most likely structure (peak shape correlation was presented in square) and N_2-methyl-L-Lys was also proposed as a potential candidate due to structure similarity. Extracted Ion Chromatograms (EIC) for DI *m/z* 84.0811 for the sample measured at 200 V. Peaks were matched and retrieved with our in-house fragment library from CMM for L-Lys derivatives identification considering experimental RMT (tolerance 6%) and $[M+H]^+$ (tolerance 10 ppm). Step 2, Experimental ISF MS spectrum for $MAAH^+$ unknown candidate was compared with *in-silico* MS/MS predictions from reference libraries and with ISF spectra of authentic standards. Note that the predicted fragmentation pattern displayed a fragment ion at m/z 115.1235 which is not experimentally observed as the base peak, since all mechanistic evidences indicates that the immonium ion $[M+H-H_2O-CO]^+$ coming from Pathway a.1 is not the major fragmentation pathway when protonation site is on a basic atom on the side-chain group. Step 3, See the explained fragmentation mechanisms in the Case Study 2 (Figure 4). Step 3, Structure validation with authentic standards.

Case Study 3. Targeted MAAs analysis based on diagnostic ion in human plasma

Step 1

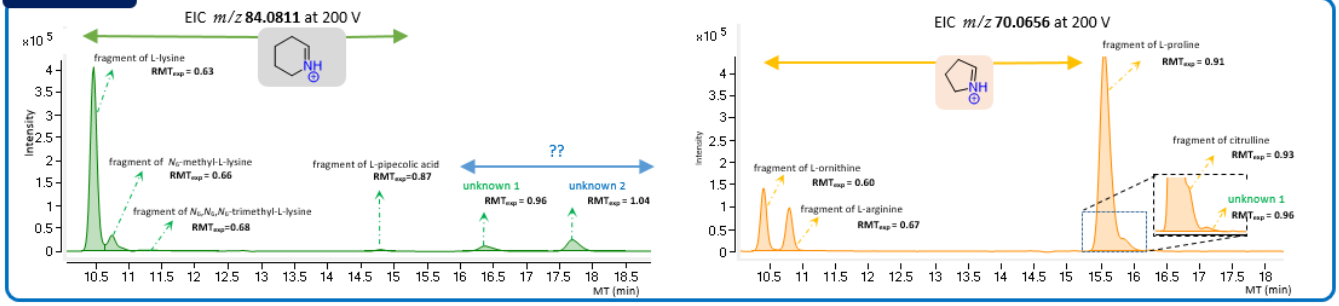

Step 2

CEU Mass Mediator

- Extract experimental IS-CID MS unknowns spectra at 200 V
- Follow Fig 1. for peak identification in Methods to confirm **[M+H]⁺**
- Compare the experimental **[M+H]⁺** to databases to generate putative identities
- Compare against predicted low-energy MS/MS CID spectra in the databases
- Discard structure candidates from putative identities without the **diagnostic ions**
- Choose best fragment matching and diagnostic ion as the base peak

Top candidates

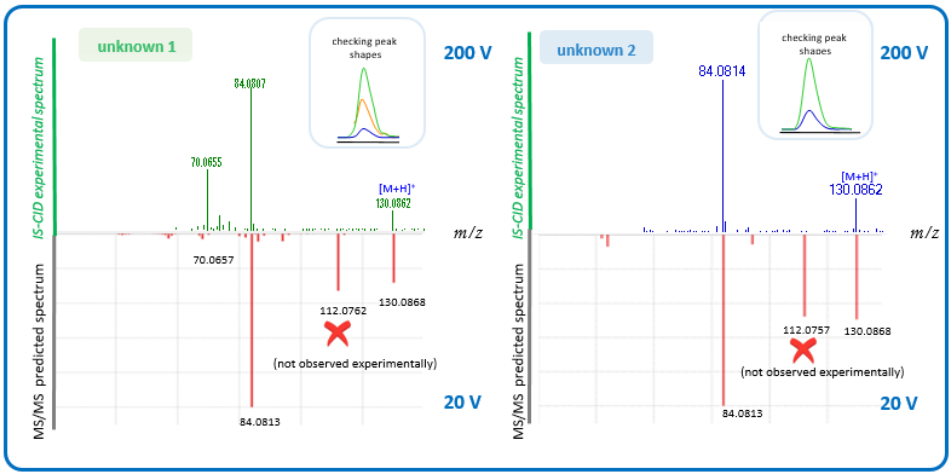

L-*trans*-4-methyl-2-pyrrolidinecarboxylic acid — **N-methyl-L-proline**

Step 3

- Study of AAs fragmentation mechanisms for structural assignment
- Integrate the knowledge of fragmentation mechanism with database searches

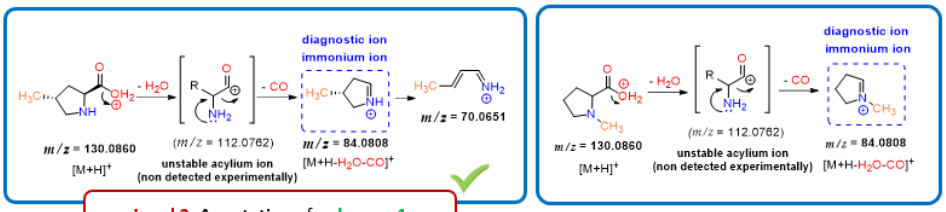

Level 2: Annotation of **unknown 1**

Step 4 **Validation**

Metabolite identification confidence levels

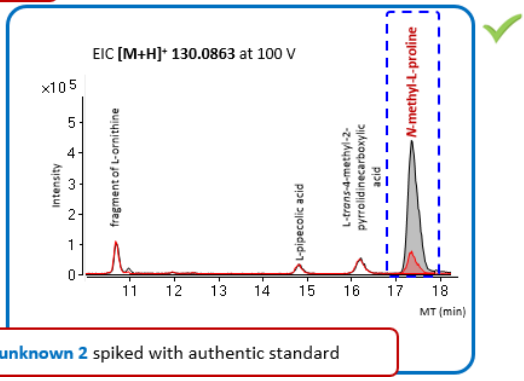

Level 1: Identification of **unknown 2** spiked with authentic standard

Figure S14. Case Study 3. Targeted MAAs analysis based on diagnostic ions in human plasma sample. Step 1, In this illustrative example, the extracted DIs m/z 84.0811 and m/z 70.0655 had multiple hits. Structures were matched and retrieved from CMM for compounds identification considering experimental RMT and $[M+H]^+$. Step 2, For each unknown the fragmentation pattern of ISF experimental data, displayed on the upper half of each mass spectrum was compared with *in silico* predicted peaks from low energy MS/MS spectra for putative candidates, displayed on the lower half. Peak shape correlation was presented in squares. *N*-methyl-L-proline and L-*trans*-4-methyl-2-pyrrolidinecarboxylic acid were retrieve from low energy MS/MS spectra from reference libraries and were ranked as the most likely structure candidates. The predicted MS/MS data were matched with our experimental IS-CID spectra for fragmentation comparison. Due to the structural similarities between these two metabolites it can lead to false annotation. Step 3, When mechanism was integrated in the identification only *N*-methyl-L-proline showed a rational sense. Note that the predicted fragmentation pattern displayed a fragment ion at m/z 112.0757 which is never experimentally observed since all evidences indicates that the acylium ions $[M+H-H_2O]^+$ formed are unstable and exothermically eliminate CO to form $[M+H-H_2O-CO]^+$ (Pathway a.1.). Step 4, Depending on the availability of standards and the information in databases, the identification outcome may have different levels of confidence. These differences led to the establishment of the confidence classification system. The first classification, set by the Chemical Analysis Working Group (CAWG) of the Metabolomics Standards Initiative (MSI) [16] including five confidence levels which have been recently reviewed by Schrimpe-Rutledge et al. [17] Lastly, *N*-methyl-L-proline was successfully validated spiking the sample with the authentic standard.

Supporting Spectra S1-S20 Compilation of all fragmentation spectra setting the fragmentor voltage at 100 and 200 V for 20 proteinogenic L-amino acids.

Spectra group 1: L-glycine

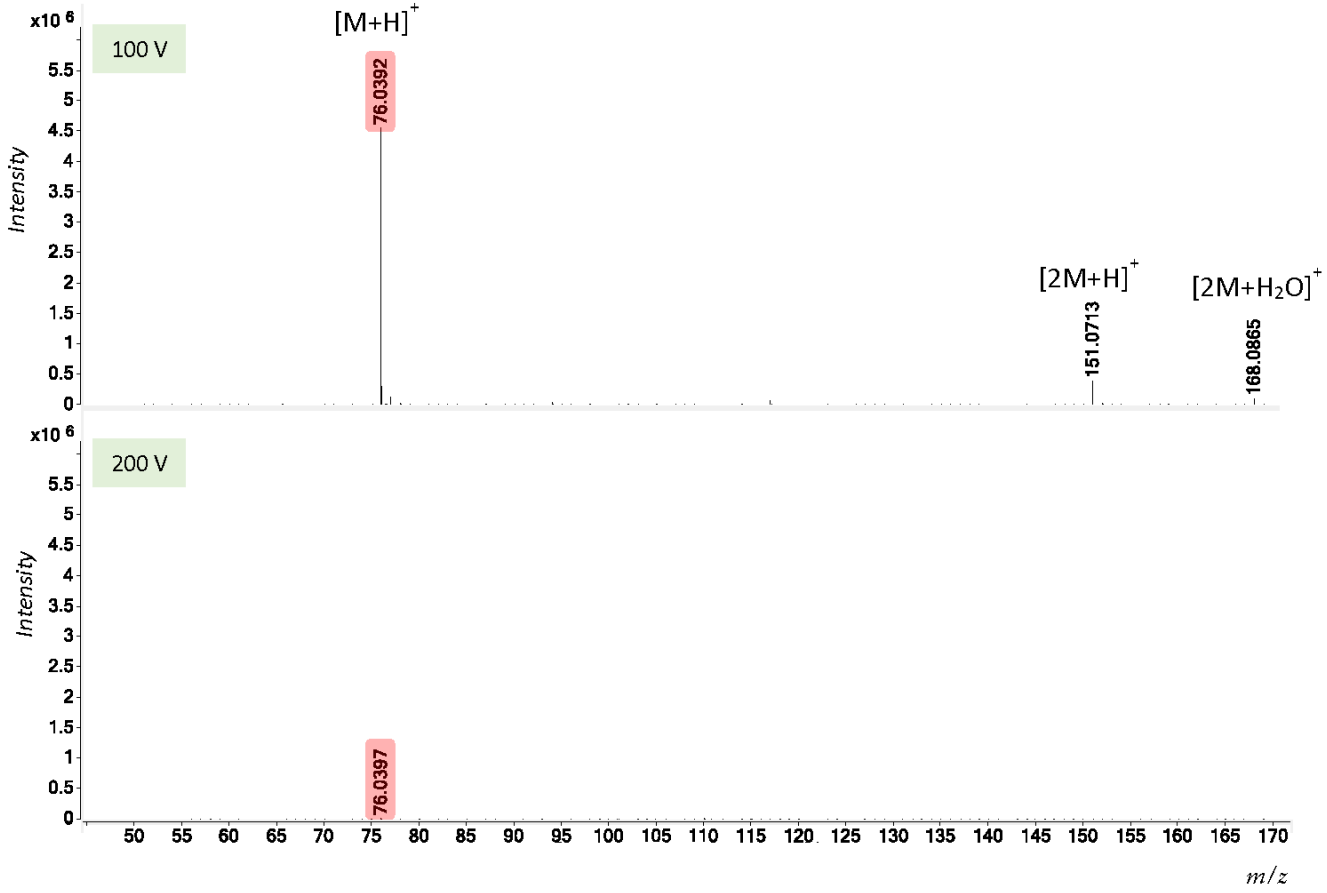

Spectra group 1: L-alanine

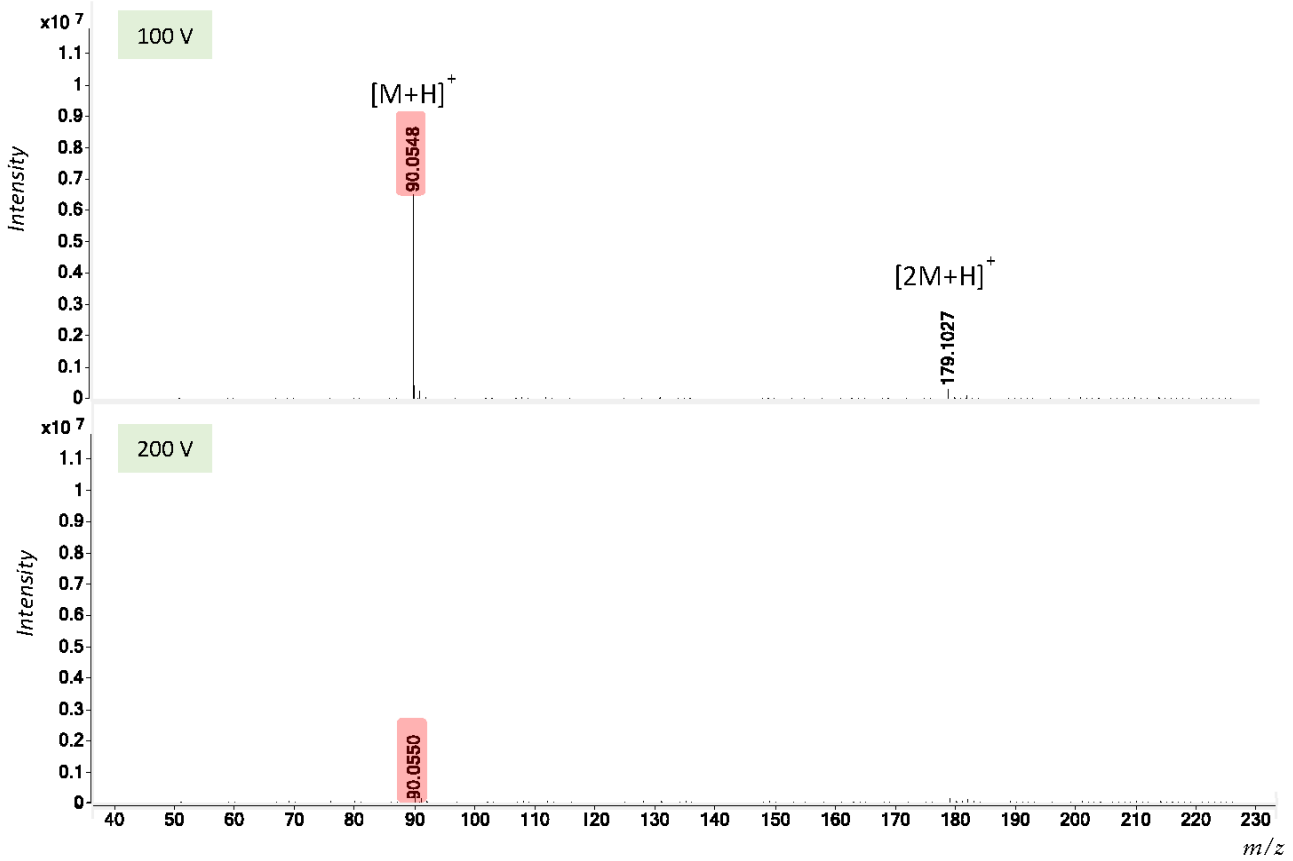

Spectra group 1: L-proline

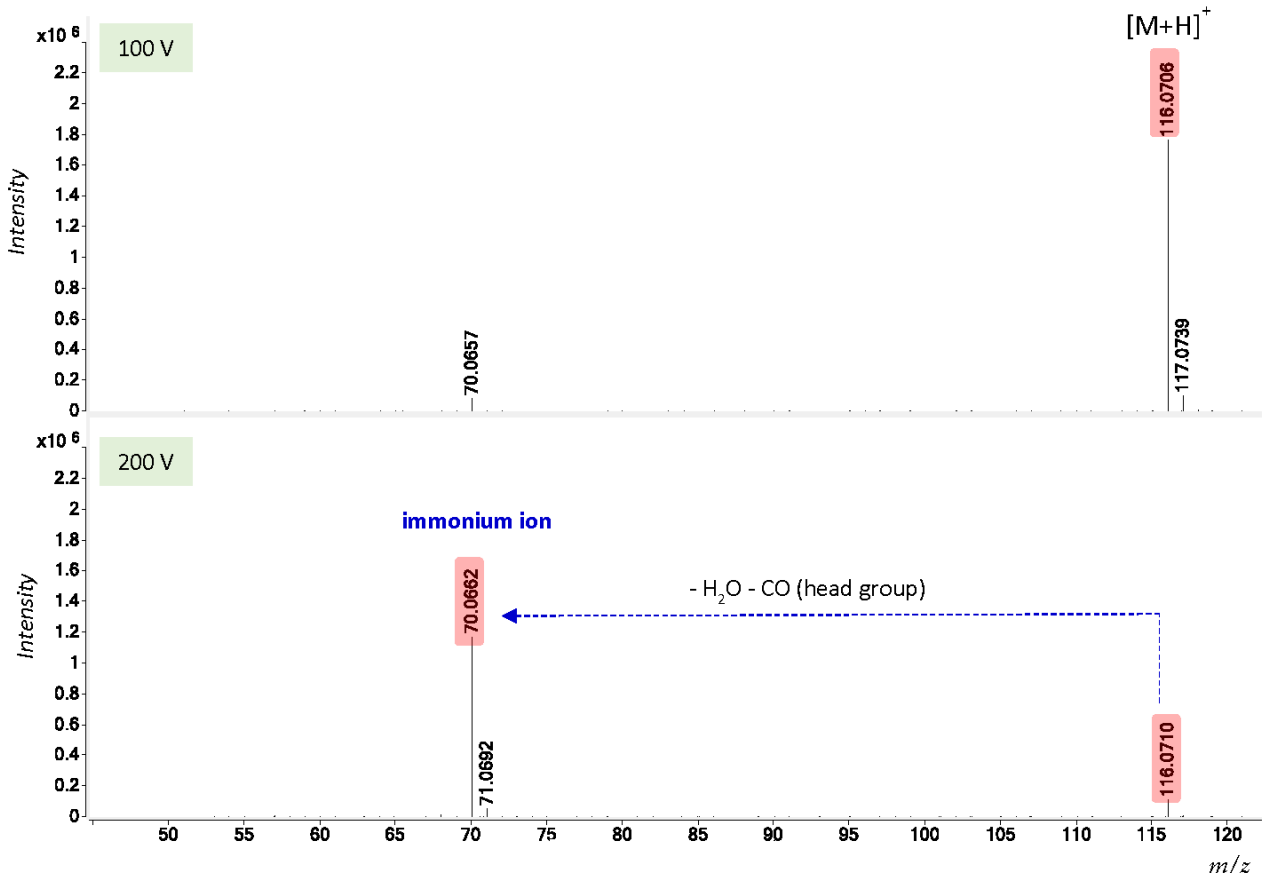

Spectra group 1: L-valine

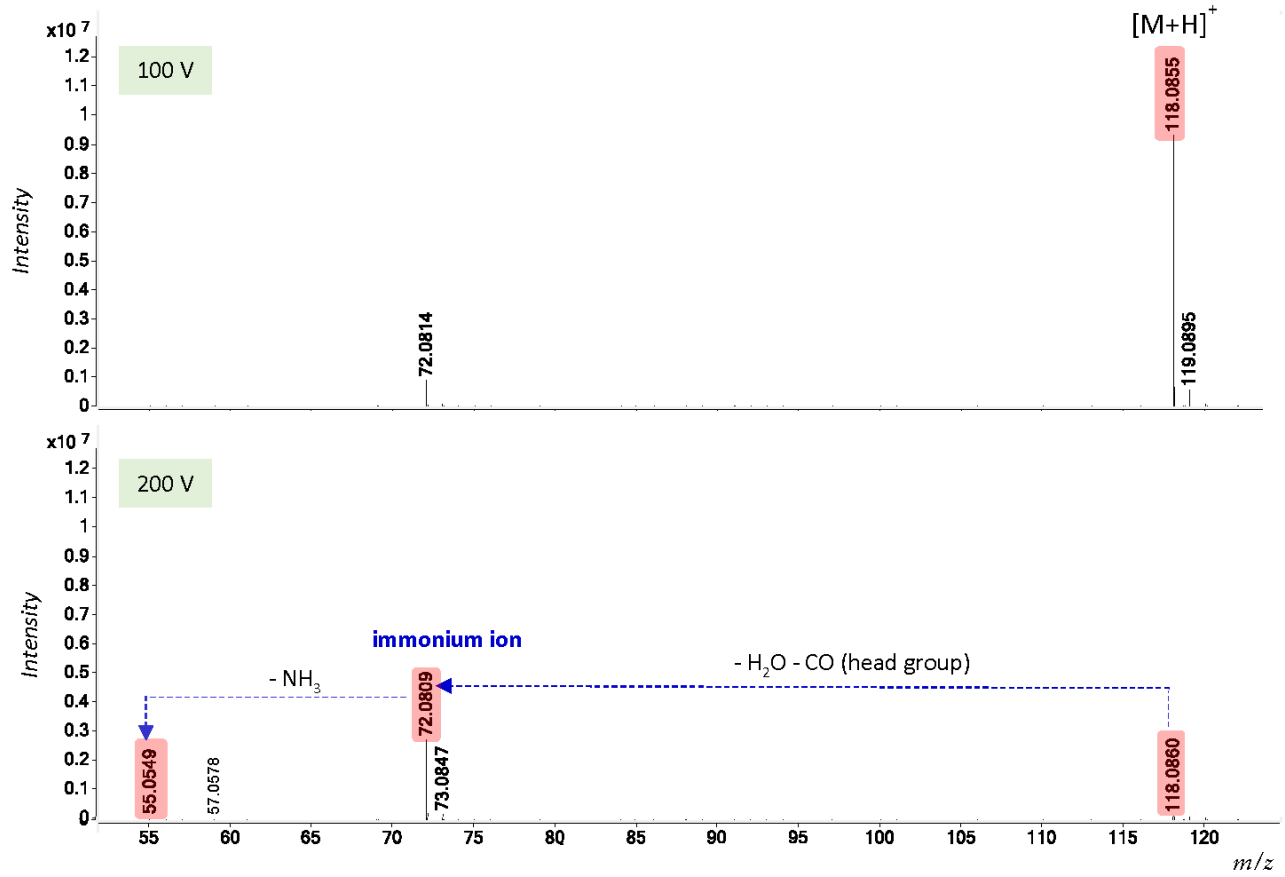

Spectra group 1: L-leucine

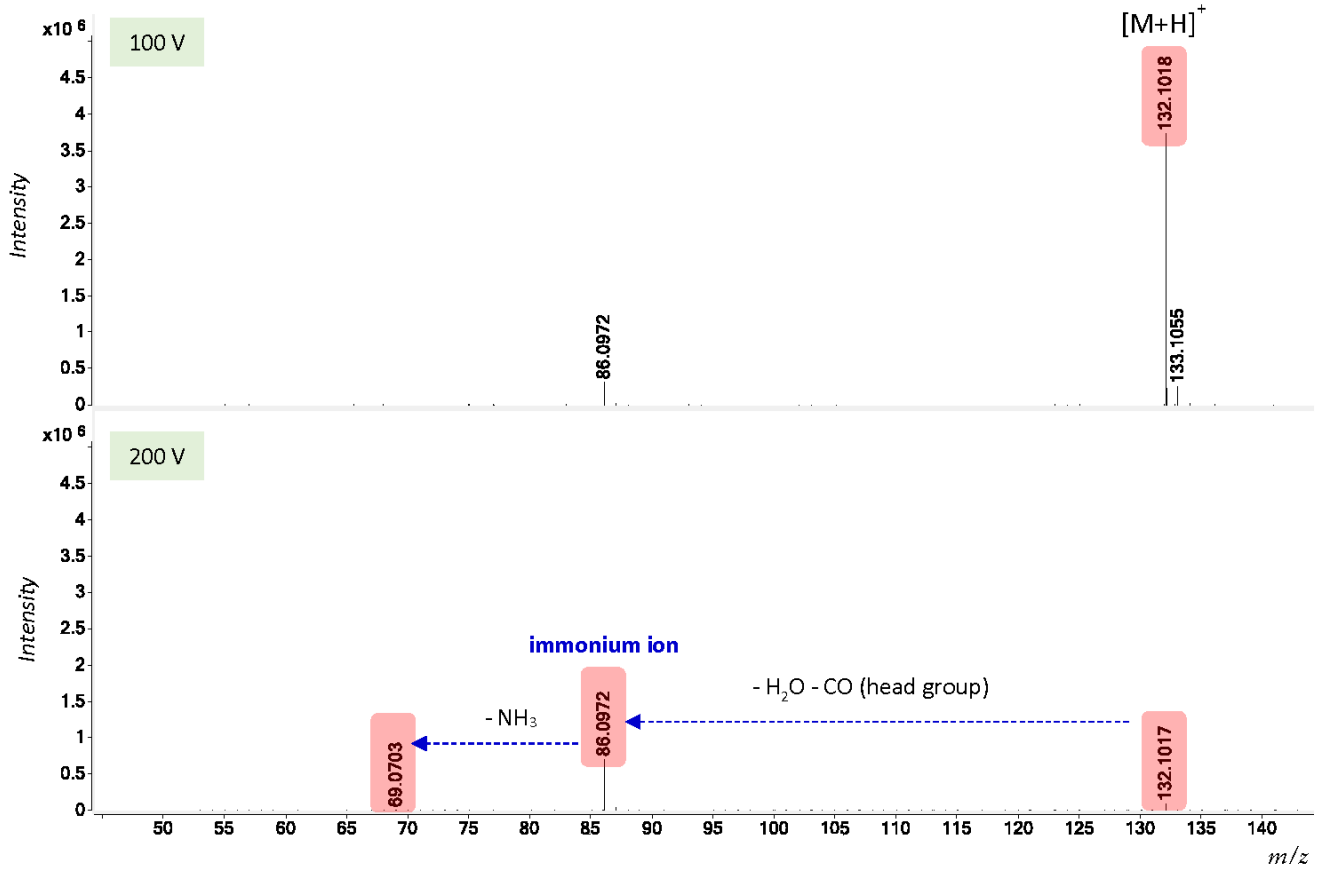

Spectra group 1: L-isoleucine

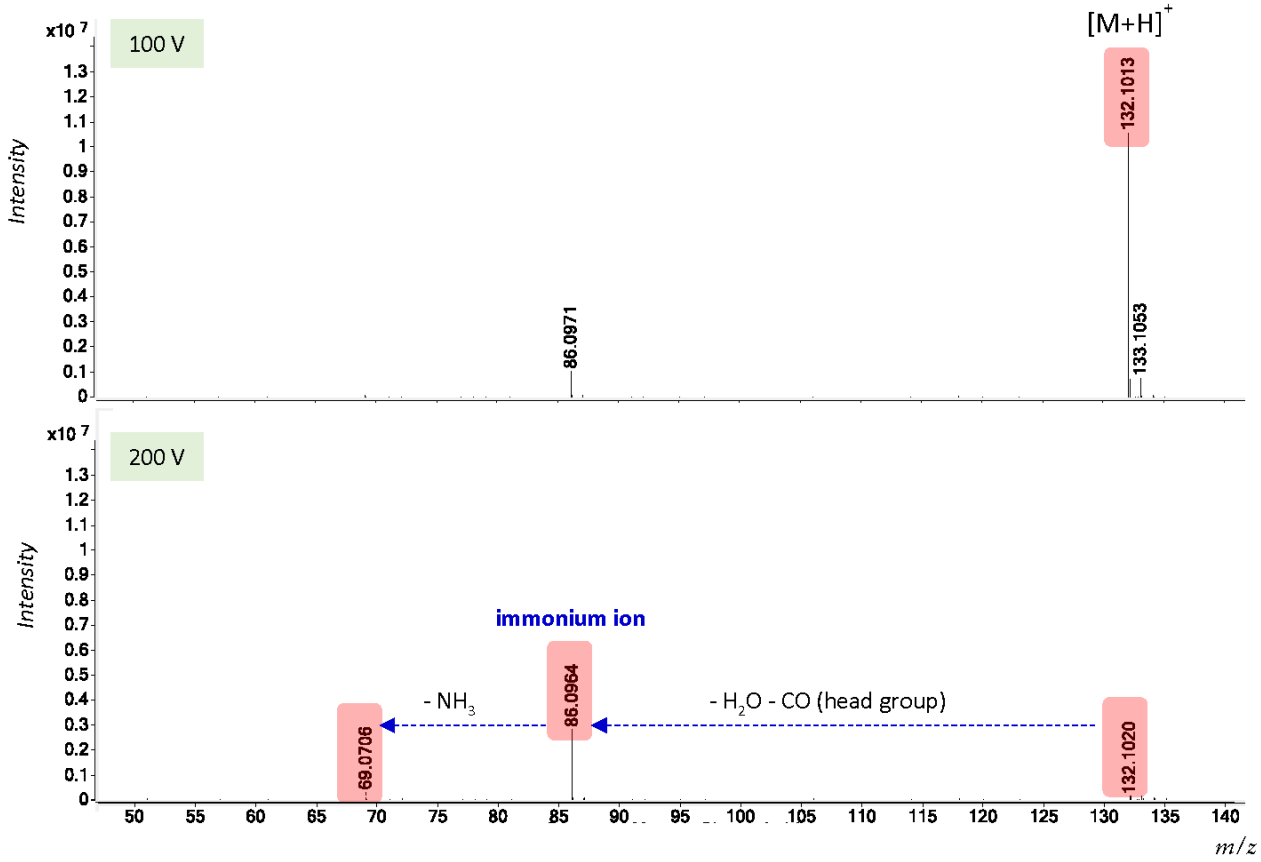

Spectra group 2: L-histidine

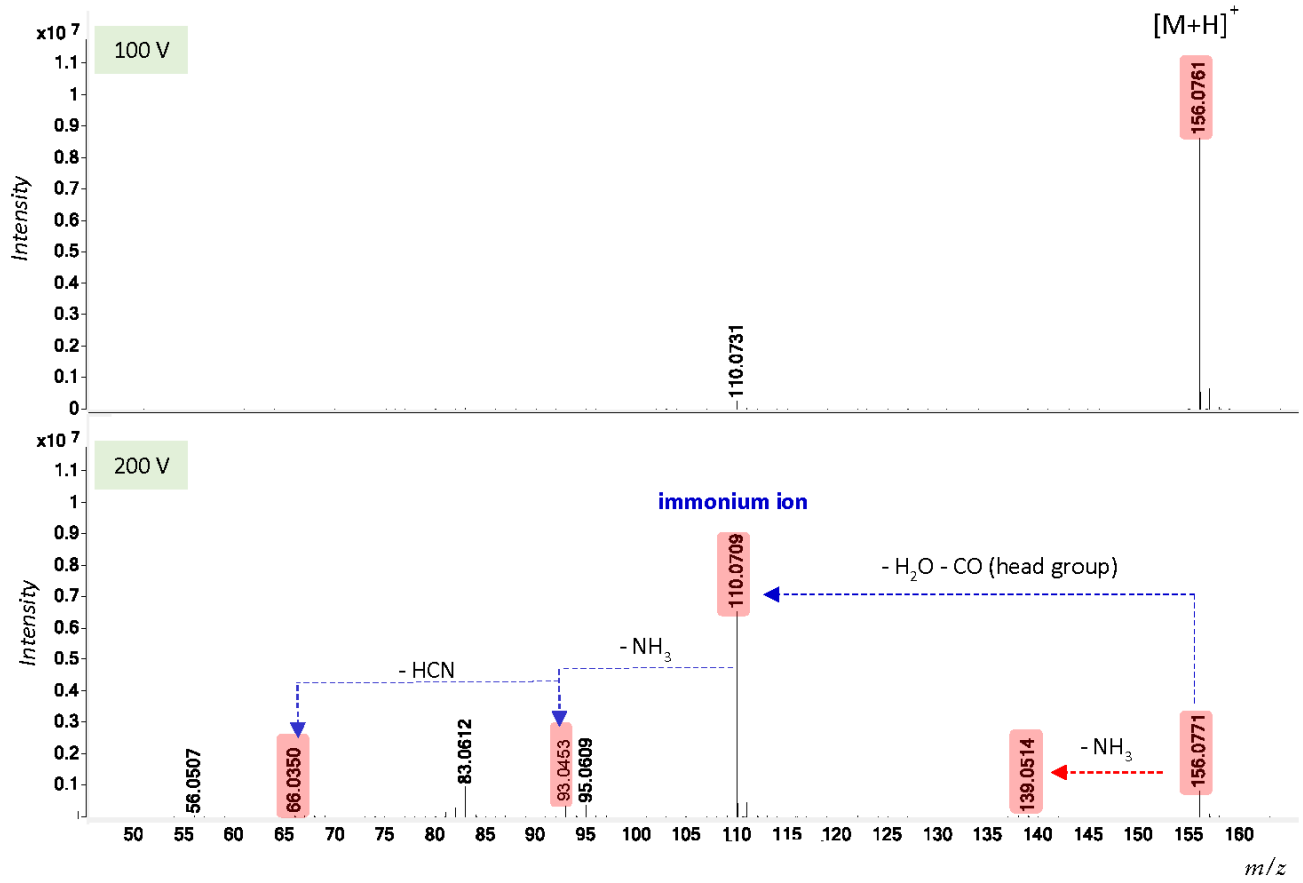

Spectra group 2: L-phenylalanine

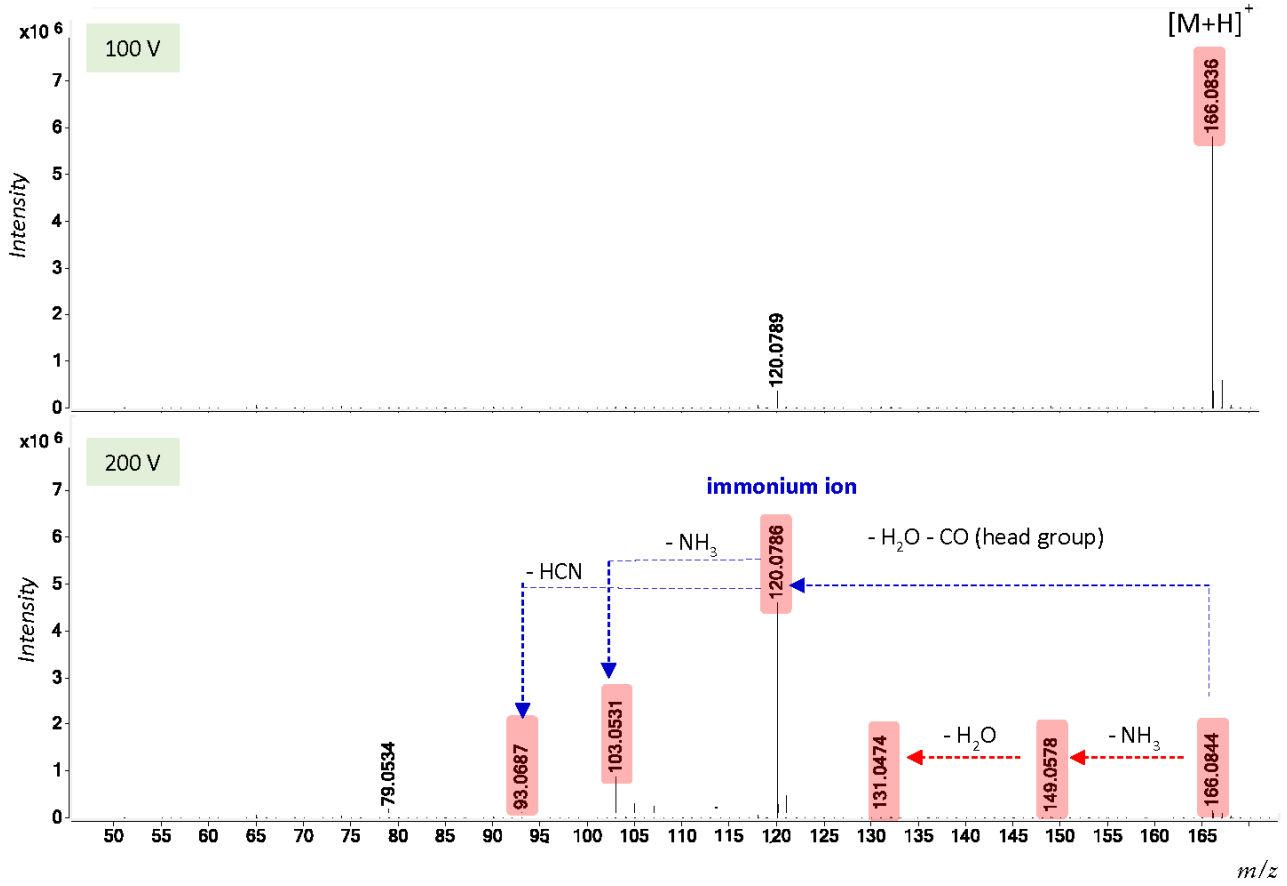

Spectra group 2: L-tyrosine

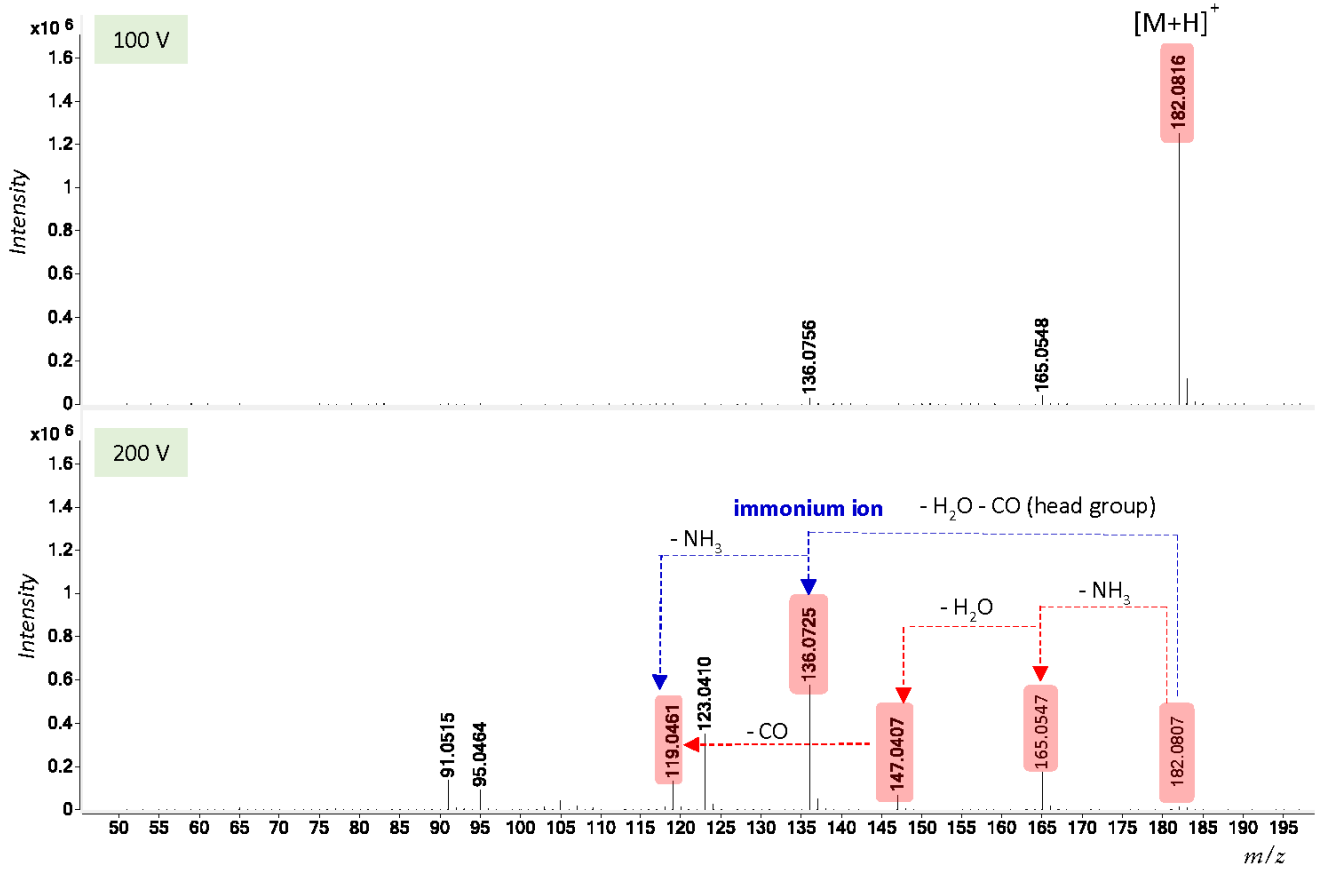

Spectra group 2: L-tryptophan

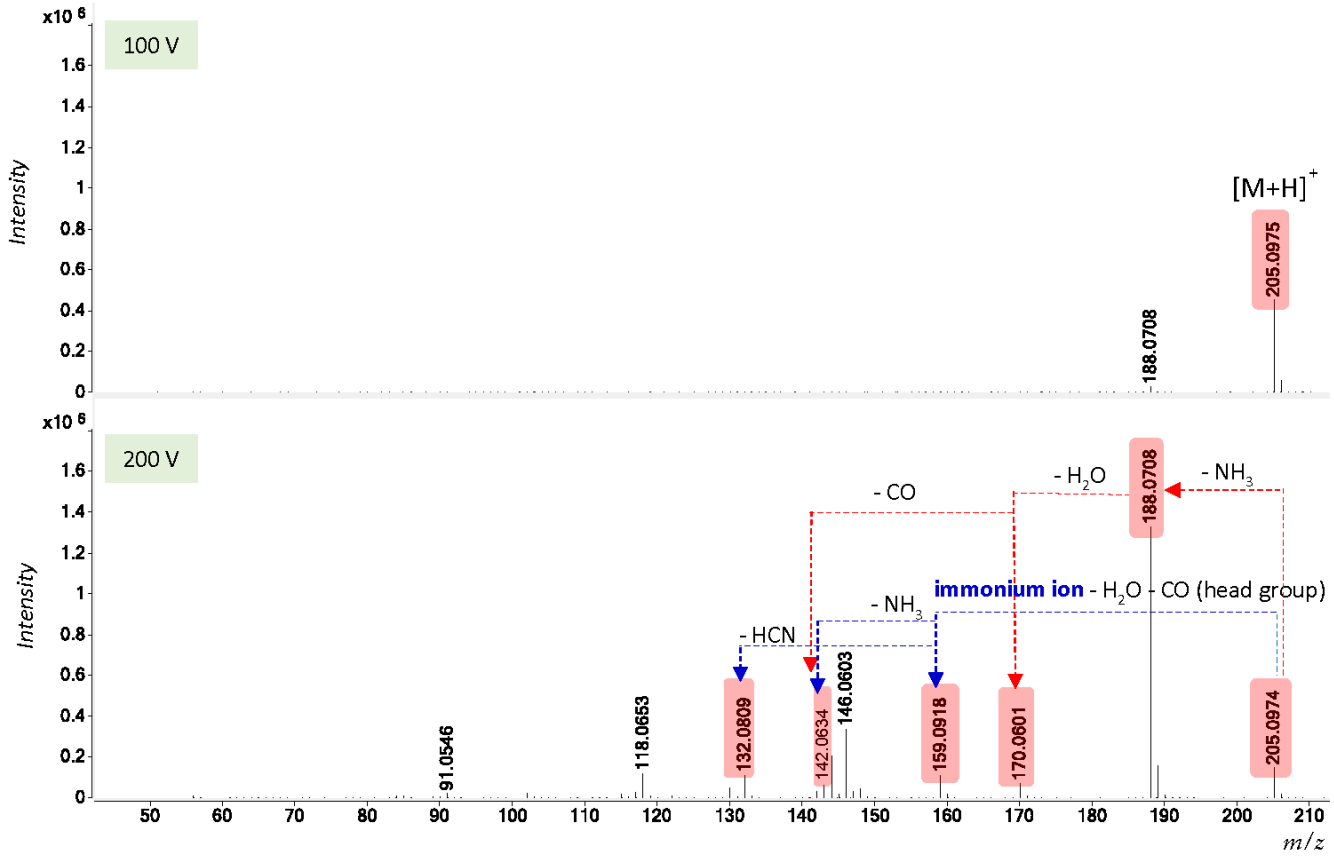

Spectra group 3: L-cysteine

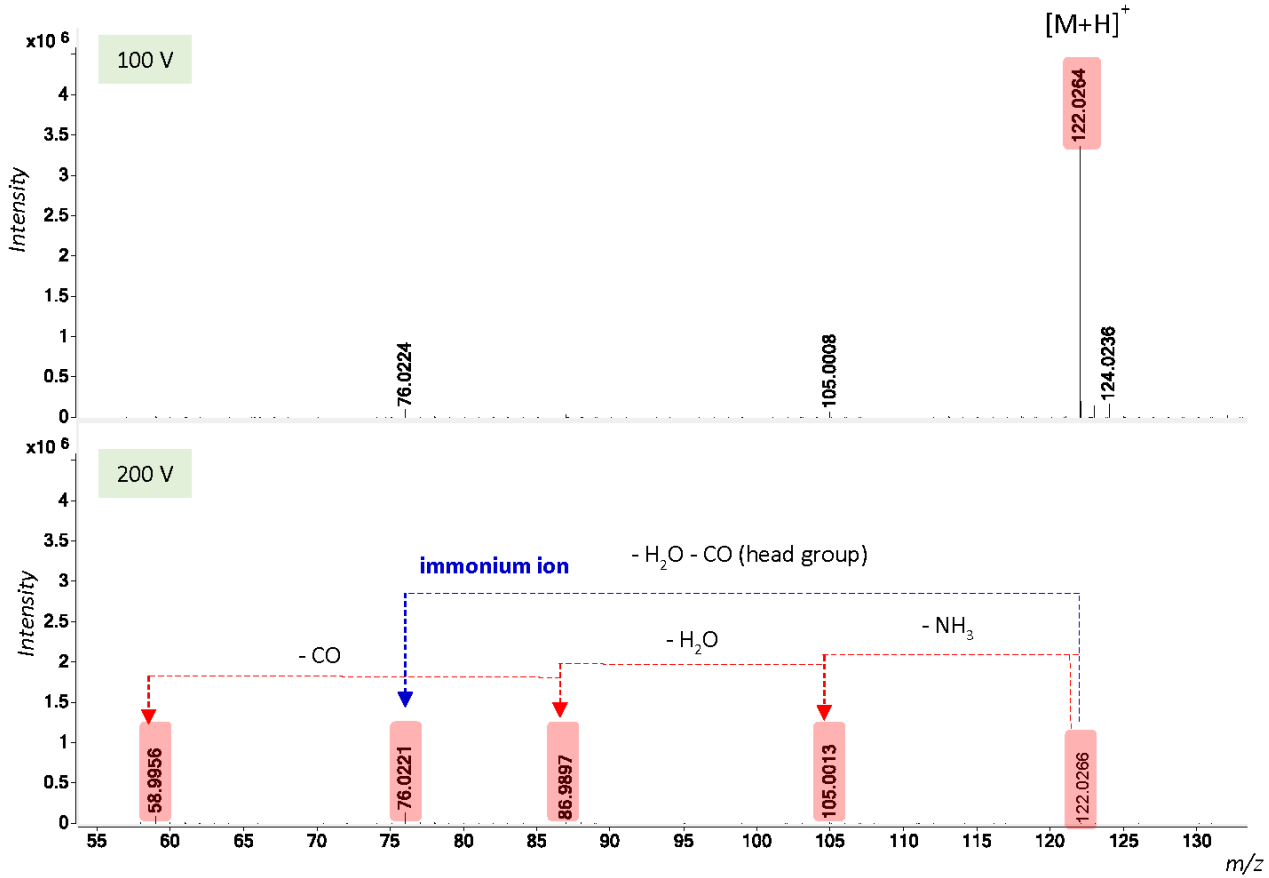

Spectra group 3: L-methionine

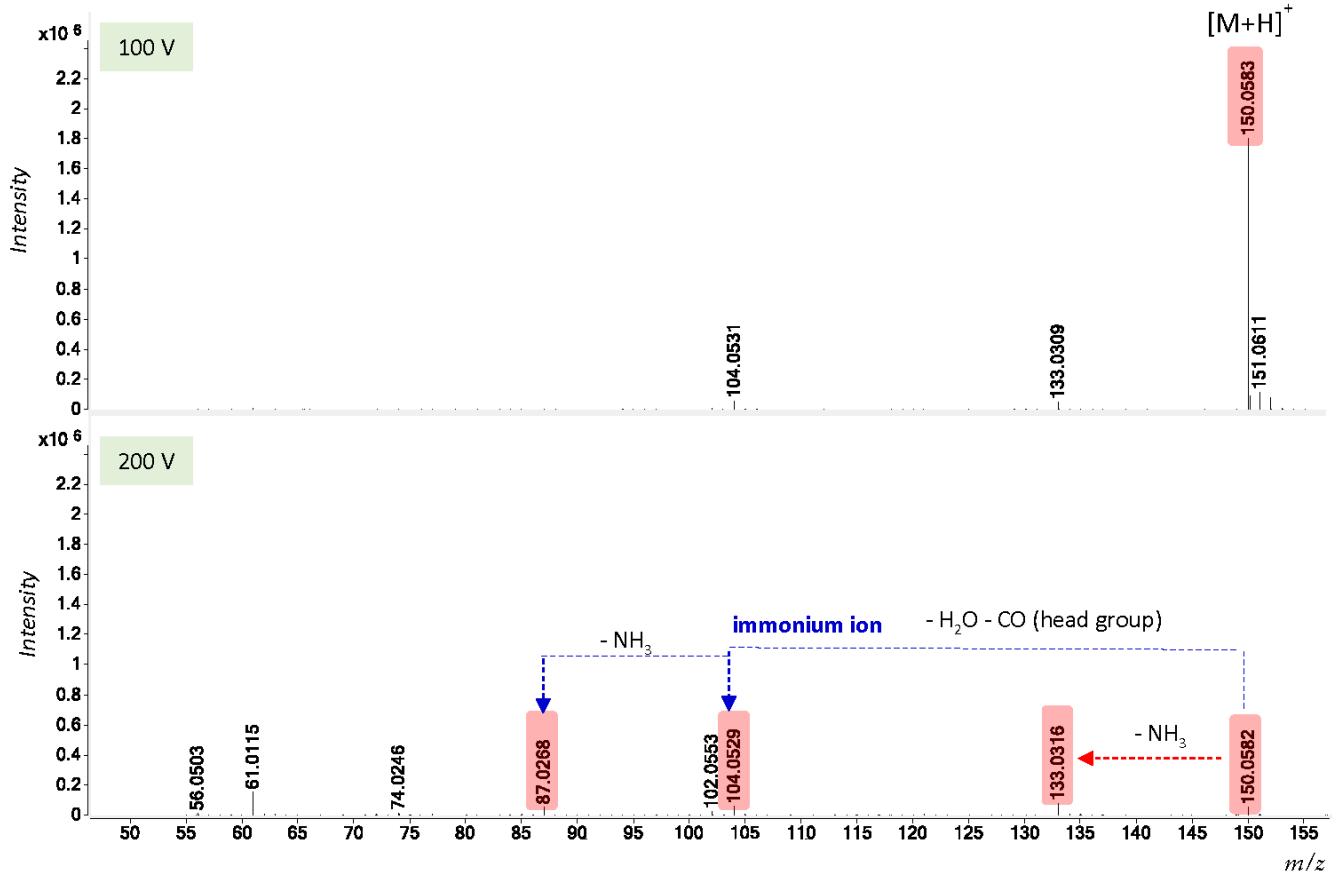

Spectra group 3: L-asparagine

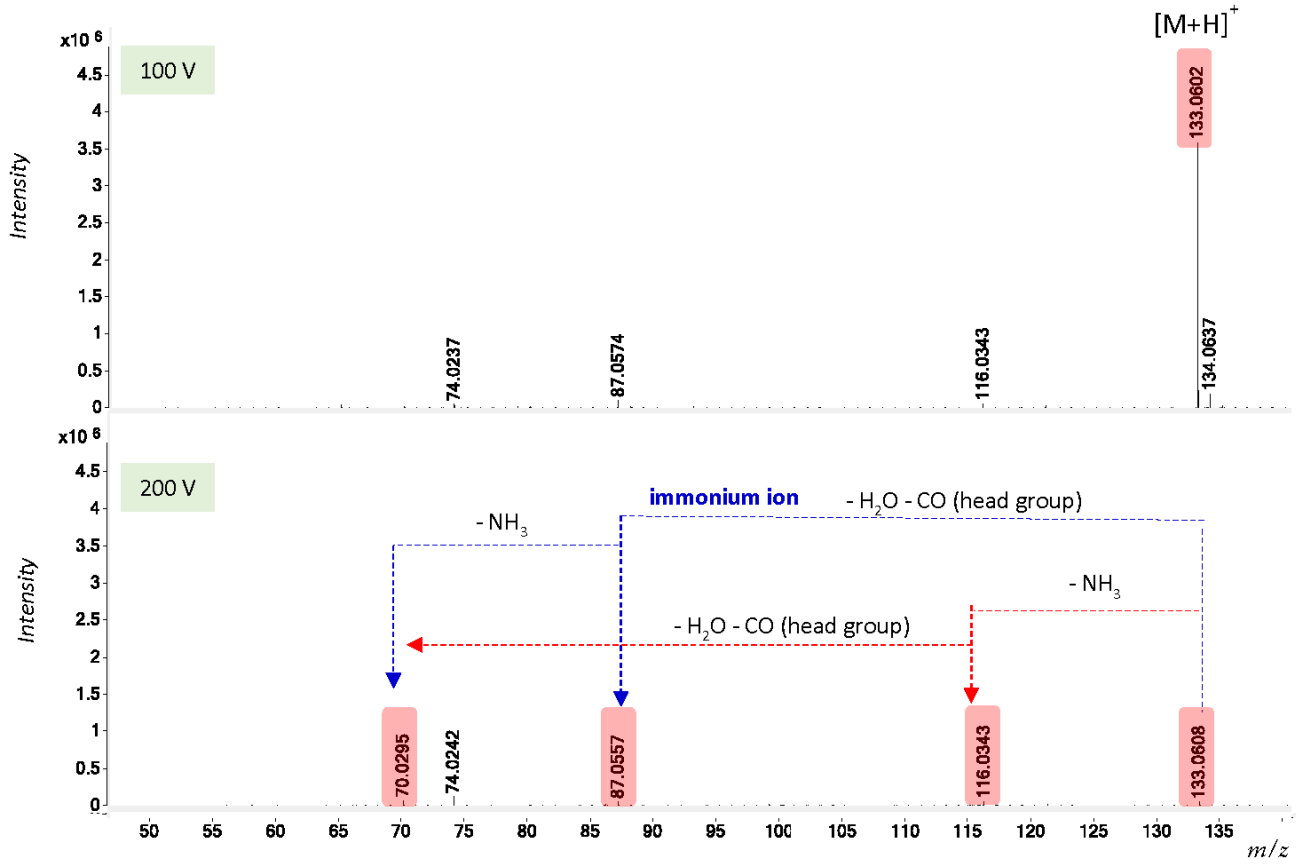

Spectra group 3: L-glutamine

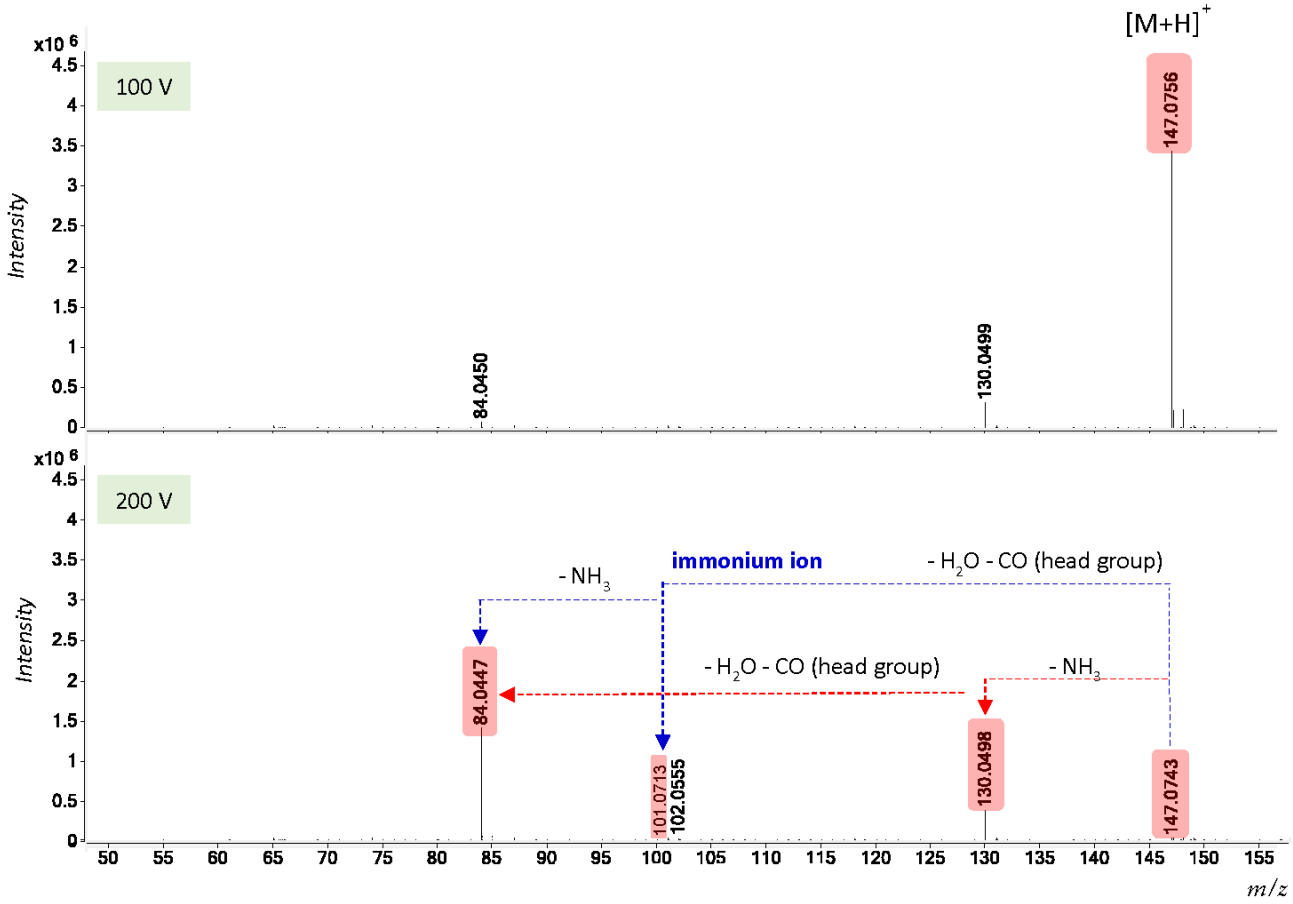

Spectra group 4: L-serine

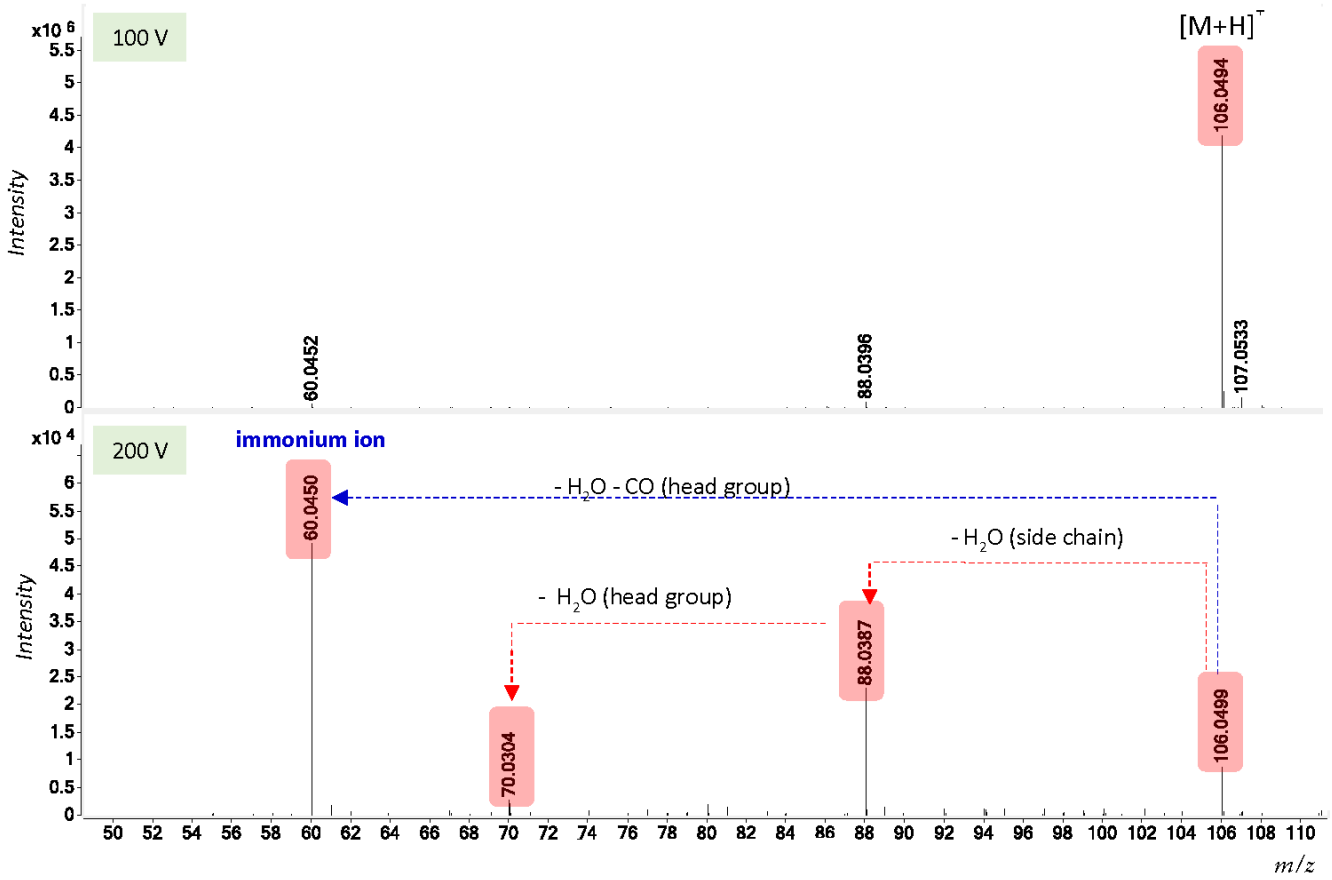

Spectra group 4: L-threonine

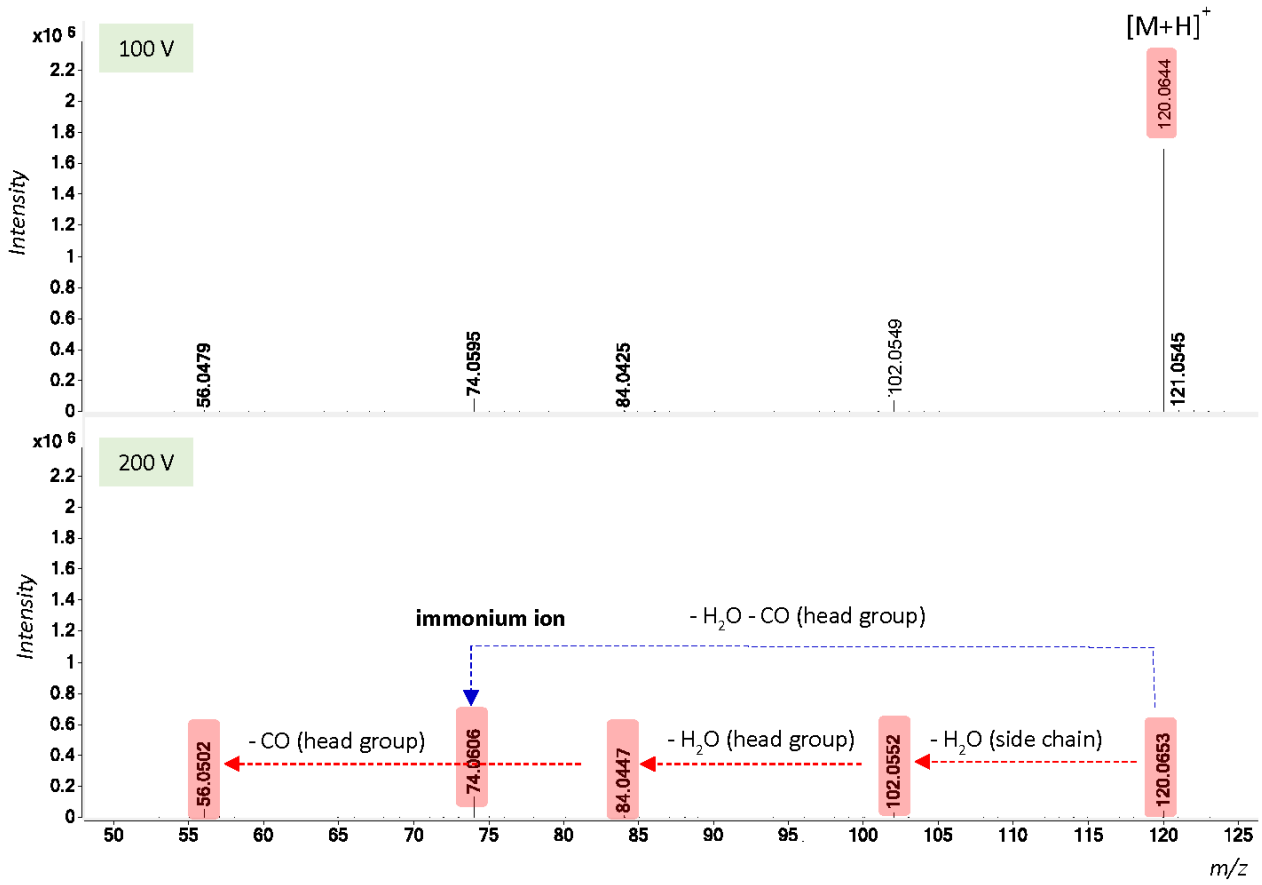

Spectra group 4: L-aspartic acid

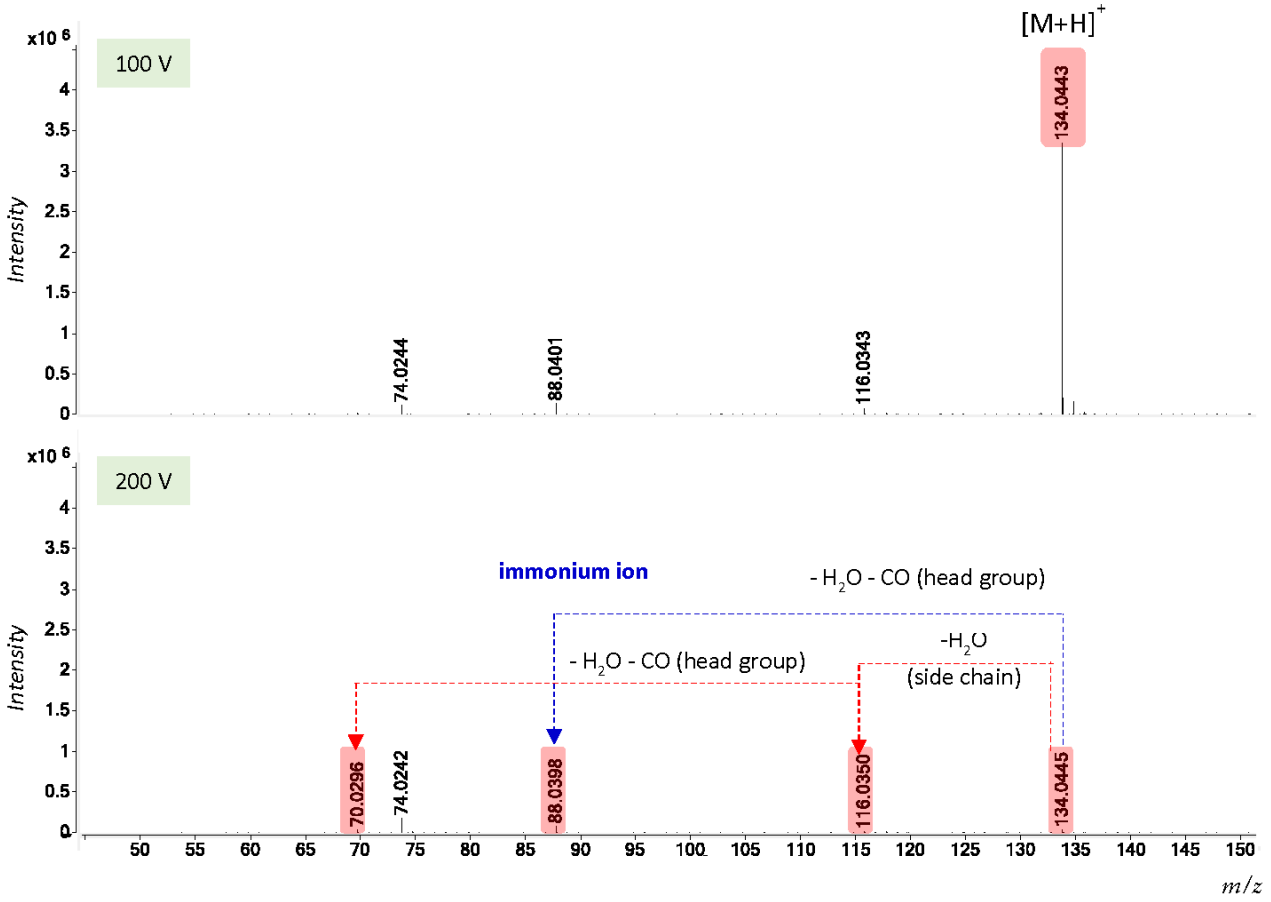

Spectra group 4: L-glutamic acid

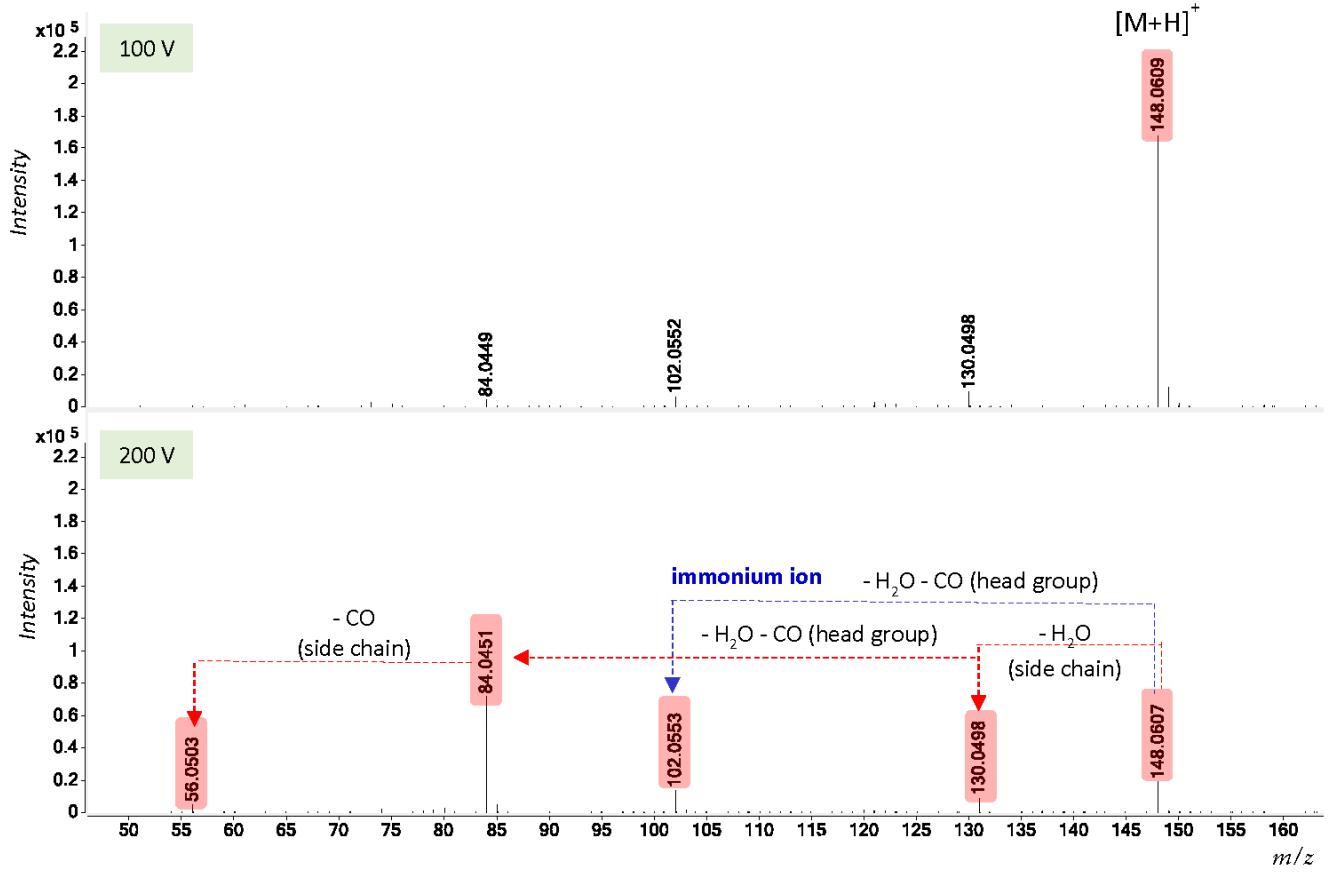

Spectra group 5: L-lysine

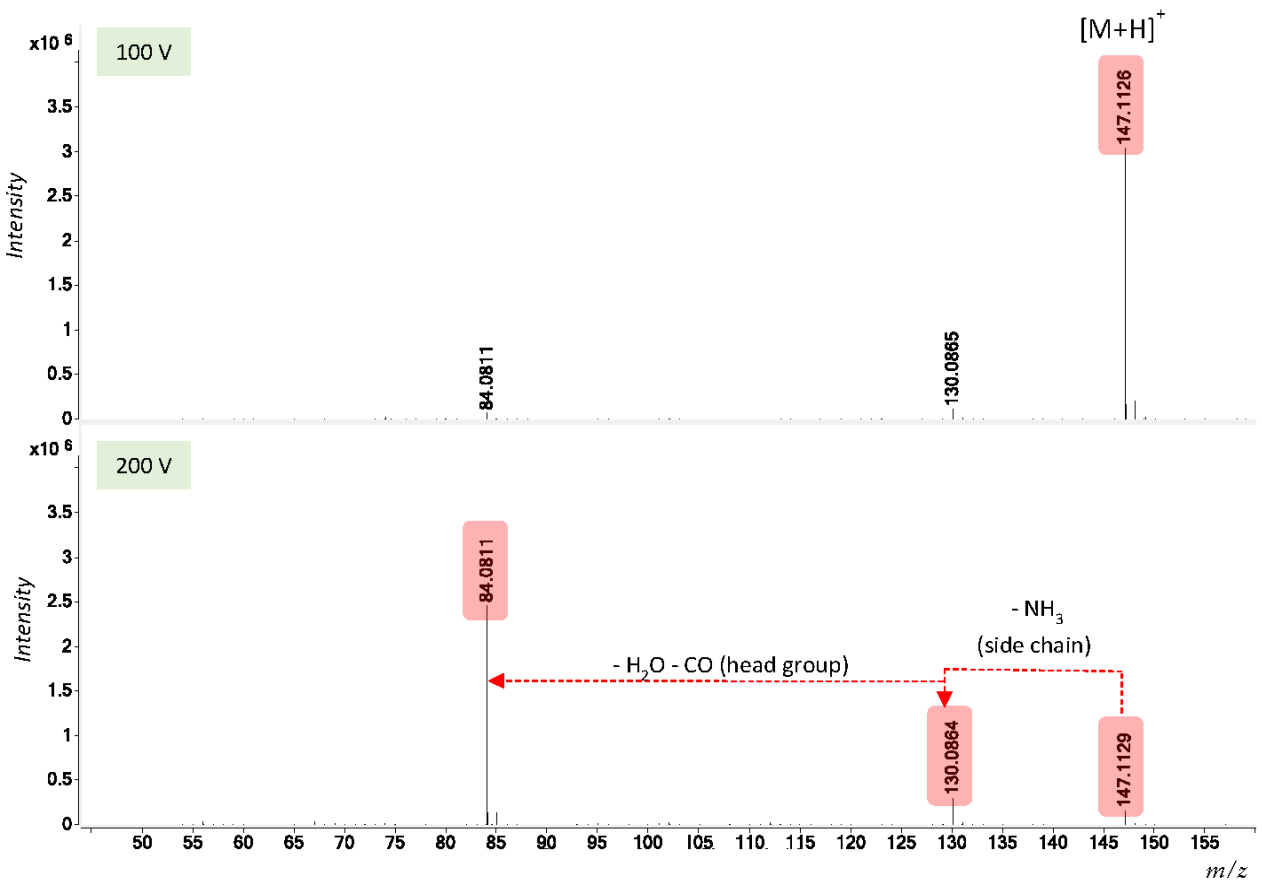

Spectra group 5: L-arginine